



CMS-HIN-14-002

CERN-PH-EP/2013-037
2015/02/03

Long-range two-particle correlations of strange hadrons with charged particles in pPb and PbPb collisions at LHC energies

The CMS Collaboration^{*}

Abstract

Measurements of two-particle angular correlations between an identified strange hadron (K_S^0 or $\Lambda/\bar{\Lambda}$) and a charged particle, emitted in pPb collisions, are presented over a wide range in pseudorapidity and full azimuth. The data, corresponding to an integrated luminosity of approximately 35 nb^{-1} , were collected at a nucleon-nucleon center-of-mass energy ($\sqrt{s_{NN}}$) of 5.02 TeV with the CMS detector at the LHC. The results are compared to semi-peripheral PbPb collision data at $\sqrt{s_{NN}} = 2.76\text{ TeV}$, covering similar charged-particle multiplicities in the events. The observed azimuthal correlations at large relative pseudorapidity are used to extract the second-order (v_2) and third-order (v_3) anisotropy harmonics of K_S^0 and $\Lambda/\bar{\Lambda}$ particles. These quantities are studied as a function of the charged-particle multiplicity in the event and the transverse momentum of the particles. For high-multiplicity pPb events, a clear particle species dependence of v_2 and v_3 is observed. For $p_T < 2\text{ GeV}$, the v_2 and v_3 values of K_S^0 particles are larger than those of $\Lambda/\bar{\Lambda}$ particles at the same p_T . This splitting effect between two particle species is found to be stronger in pPb than in PbPb collisions in the same multiplicity range. When divided by the number of constituent quarks and compared at the same transverse kinetic energy per quark, both v_2 and v_3 for K_S^0 particles are observed to be consistent with those for $\Lambda/\bar{\Lambda}$ particles at the 10% level in pPb collisions. This consistency extends over a wide range of particle transverse kinetic energy and event multiplicities.

Published in Physics Letters B as doi:10.1016/j.physletb/2015.01.034.

1 Introduction

Studies of multiparticle correlations provide important insights into the underlying mechanism of particle production in high-energy collisions of protons and nuclei. A key feature of such correlations in ultrarelativistic nucleus-nucleus (AA) collisions is the observation of a pronounced structure on the near side (relative azimuthal angle $|\Delta\phi| \approx 0$) that extends over a large range in relative pseudorapidity ($|\Delta\eta|$ up to 4 units or more). This feature, known as the “ridge”, has been found over a wide range of AA energies and system sizes at both the Relativistic Heavy Ion Collider (RHIC) [1–5] and the Large Hadron Collider (LHC) [6–10] and is interpreted as arising primarily from the collective hydrodynamic flow of a strongly interacting, expanding medium [11, 12].

Similar long-range correlations have also been discovered in proton-proton (pp) [13], proton-lead (pPb) [14–16], and deuteron-gold (dAu) [17] collisions with high final-state particle multiplicity. As the collision volume size is reduced, it is possible that the system will not be able to equilibrate and the hydrodynamic description will break down. As such, there has been no consensus on the origin of the particle correlation structure in these smaller systems. A variety of theoretical models have been proposed to interpret this phenomenon in pp [18], pPb, and dAu collisions. Besides hydrodynamic effects in a high-density system [19, 20], an alternate model including gluon saturation in the incoming nucleons has also been shown to describe these data [21, 22].

In hydrodynamical descriptions, the collective flow manifests itself as an azimuthal anisotropy in the distribution of final-state particles. An additional key consequence of these models is that the measured anisotropies will depend on the mass of the particle [23–25]. More specifically, for particles with transverse momentum below about 2 GeV, the anisotropy will be larger for lighter particles. The presence of this mass ordering is well established in AA collisions at RHIC and LHC energies [26–30]. This phenomenon has recently also been observed in pPb [31] and dAu [17] collisions, consistent with expectations from hydrodynamic models [32, 33]. The analysis presented in this paper aims to further explore this effect by extracting anisotropies of identified strange mesons (K_S^0) and baryons (Λ and $\bar{\Lambda}$) in pPb and in PbPb collisions that produce similar final-state particle multiplicity.

The azimuthal correlations of emitted particle pairs are typically characterized by their Fourier components, $\frac{dN_{\text{pair}}}{d\Delta\phi} \propto 1 + \sum_n 2V_{n\Delta} \cos(n\Delta\phi)$, where $V_{n\Delta}$ are the two-particle Fourier coefficients and $v_n = \sqrt{V_{n\Delta}}$ denote the single-particle anisotropy harmonics [34]. In particular, the second and third Fourier components are known as elliptic (v_2) and triangular (v_3) flow, respectively [12]. In hydrodynamical models, v_2 and v_3 are directly related to the response of the medium to the initial collision geometry and its fluctuations [35–37]. As such, these Fourier components can provide insight into the fundamental transport properties of the medium.

In AA collisions at RHIC, a scaling of v_2 as a function of p_T with the number of constituent quarks (n_q) has been observed in the range $2 < p_T < 6$ GeV [38]. Specifically, the values of v_2/n_q are found to be very similar for all mesons ($n_q = 2$) and baryons ($n_q = 3$) when compared at the same value of p_T/n_q . This empirical scaling may indicate that final-state hadrons are formed through recombination of quarks in this p_T regime [39–41], possibly providing evidence of deconfinement of quarks and gluons in these systems. At lower p_T ($p_T < 2$ GeV), a similar scaling behavior is observed, although, according to perfect fluid hydrodynamics, v_2/n_q values must be compared at the same transverse kinetic energy per constituent quark (KE_T/n_q , where $KE_T = \sqrt{m^2 + p_T^2} - m$) to account for the mass difference of hadrons [42, 43].

This paper presents an analysis of two-particle correlations with identified strange hadrons, K_S^0

and $\Lambda/\bar{\Lambda}$, in pPb collisions at a center-of-mass energy per nucleon pair ($\sqrt{s_{NN}}$) of 5.02 TeV. With the implementation of a dedicated high-multiplicity trigger, the 2013 pPb data sample gives access to multiplicities comparable to those in semi-peripheral PbPb collisions. Two-particle correlation functions are constructed by associating a K_S^0 or $\Lambda/\bar{\Lambda}$ particle with a charged particle (pairs of K_S^0 or $\Lambda/\bar{\Lambda}$ particles are not studied due to their limited statistical precision). In the context of hydrodynamic models, Fourier coefficients of dihadron correlations can be factorized into products of single-particle azimuthal anisotropies. Assuming that this relationship holds, v_2 and v_3 are extracted from long-range two-particle correlations as a function of strange hadron p_T and event multiplicity. To examine the validity of constituent quark number scaling, v_2/n_q and v_3/n_q are obtained as a function of KE_T/n_q for both K_S^0 and $\Lambda/\bar{\Lambda}$ particles. A direct comparison of the pPb and PbPb results over a broad range of similar multiplicities is presented.

2 The CMS experiment and data sample

A description of the CMS detector in the LHC at CERN can be found in Ref. [44]. The main detector component used in this paper is the tracker, located in a superconducting solenoid of 6 m internal diameter, providing a magnetic field of 3.8 T. The tracker consists of 1440 silicon pixel and 15 148 silicon strip detector modules, covering the pseudorapidity range $|\eta| < 2.5$. For hadrons with $p_T \approx 1$ GeV and $|\eta| \approx 0$, the impact parameter (distance of closest approach from the primary collision vertex) resolution is approximately 100 μm and the p_T resolution is 0.8%.

Also located inside the solenoid are the electromagnetic calorimeter (ECAL) and the hadron calorimeter (HCAL). The ECAL consists of 75 848 lead tungstate crystals, arranged in a quasi-projective geometry and distributed in a barrel region ($|\eta| < 1.48$) and two endcaps that extend to $|\eta| = 3.0$. The HCAL barrel and endcaps are sampling calorimeters composed of brass and scintillator plates, covering $|\eta| < 3.0$. Iron/quartz-fiber forward calorimeters (HF) are placed on each side of the interaction region, covering $2.9 < |\eta| < 5.2$. The detailed Monte Carlo (MC) simulation of the CMS detector response is based on GEANT4 [45].

The data sample used in this analysis was collected with the CMS detector during the LHC pPb run in 2013. The total integrated luminosity of the data set is about 35 nb^{-1} [46]. The beam energies are 4 TeV for protons and 1.58 TeV per nucleon for lead nuclei, resulting in a center-of-mass energy per nucleon pair of 5.02 TeV. The direction of the proton beam was initially set up to be clockwise (20 nb^{-1}), and was later reversed (15 nb^{-1}). As a result of the energy difference between the colliding beams, the nucleon-nucleon center-of-mass in the pPb collisions is not at rest with respect to the laboratory frame. Massless particles emitted at $\eta_{\text{cm}} = 0$ in the nucleon-nucleon center-of-mass frame will be detected at $\eta = -0.465$ (clockwise proton beam) or 0.465 (counterclockwise proton beam) in the laboratory frame. A sample of peripheral PbPb data at $\sqrt{s_{NN}} = 2.76$ TeV corresponding to an integrated luminosity of about $2.3 \mu\text{b}^{-1}$, collected during the 2011 LHC heavy-ion run, is also analyzed for comparison with pPb data at similar charged-particle multiplicity ranges.

3 Online triggering and offline track reconstruction and selection

The online triggering and the offline reconstruction and selection follow the same procedure as described in Ref. [47]. Minimum bias pPb events are triggered by requiring at least one track with $p_T > 0.4$ GeV to be found in the pixel tracker for a pPb bunch crossing. Because of hardware limits on the data acquisition rate, only a small fraction ($\sim 10^{-3}$) of all minimum bias

triggered events are recorded. In order to collect a large sample of high-multiplicity pPb collisions, a dedicated high-multiplicity trigger is also implemented using the CMS Level 1 (L1) and high-level trigger (HLT) systems. At L1, two event streams were triggered by requiring the total transverse energy summed over ECAL and HCAL to be greater than 20 or 40 GeV. Charged tracks are then reconstructed online at the HLT using the three layers of pixel detectors, and requiring a track origin within a cylindrical region of 30 cm length along the beam and 0.2 cm radius perpendicular to the beam. For each event, the number of pixel tracks ($N_{\text{trk}}^{\text{online}}$) with $|\eta| < 2.4$ and $p_T > 0.4$ GeV is counted separately for each vertex. Only tracks with a distance of closest approach of 0.4 cm or less to one of the vertices are included. The online selection requires $N_{\text{trk}}^{\text{online}}$ for the vertex with the most tracks to exceed a specific value. Data are taken with thresholds of $N_{\text{trk}}^{\text{online}} > 100, 130$ (from events with L1 threshold of 20 GeV), and 160, 190 (from events with L1 threshold of 40 GeV). While all events with $N_{\text{trk}}^{\text{online}} > 190$ are accepted, only a fraction of the events from the other thresholds are kept. This fraction is dependent on the instantaneous luminosity. Data from both the minimum bias trigger and high-multiplicity trigger are retained for offline analysis.

In the offline analysis, hadronic collisions are selected by the presence of at least one tower with energy above 3 GeV in each of the two HF calorimeters. Events are also required to contain at least one reconstructed primary vertex within 15 cm of the nominal interaction point along the beam axis and within 0.15 cm transverse to the beam trajectory. At least two reconstructed tracks are required to be associated with the primary vertex, a condition that is important only for minimum bias events. Beam related background is suppressed by rejecting events for which less than 25% of all reconstructed tracks pass the *high-purity* selection (as defined in Ref. [48]). The pPb instantaneous luminosity provided by the LHC in the 2013 run resulted in a 3% probability of having at least one additional interaction present in the same bunch crossing (pile-up events). The procedure used for rejecting pile-up events is described in Ref. [47] and is based on the number of tracks associated with each reconstructed vertex and the distance between different vertices. A purity of 99.8% for single pPb collision events is achieved for the highest multiplicity pPb interactions studied in this paper. With the selection criteria above, 97–98% of the events are found to be selected among those pPb interactions simulated with the EPOS LHC [49] and HIJING 2.1 [50] event generators that have at least one particle from the pPb interaction with energy $E > 3$ GeV in each of the η ranges $-5 < \eta < -3$ and $3 < \eta < 5$.

In this analysis, *high-purity* tracks are used to select primary tracks (tracks originating from the pPb interaction). Additional requirements are applied to enhance the purity of primary tracks. The significance of the separation along the beam axis (z) between the track and the best vertex, $d_z/\sigma(d_z)$, and the significance of the impact parameter relative to the best vertex transverse to the beam, $d_T/\sigma(d_T)$, must be less than 3, and the relative p_T uncertainty, $\sigma(p_T)/p_T$, must be less than 10%. To ensure high tracking efficiency and to reduce the rate of misreconstructed tracks, primary tracks with $|\eta| < 2.4$ and $p_T > 0.3$ GeV are used in the analysis (a p_T cutoff of 0.4 GeV is used in the multiplicity determination to match the HLT requirement). Based on simulation studies using GEANT4 to propagate particles from the HIJING event generator, the combined geometrical acceptance and efficiency for primary track reconstruction exceeds 60% for $p_T \approx 0.3$ GeV and $|\eta| < 2.4$. The efficiency is greater than 90% in the $|\eta| < 1$ region for $p_T > 0.6$ GeV. For the event multiplicity range studied in this paper, no dependence of the tracking efficiency on multiplicity is found and the rate of misreconstructed tracks is 1–2%.

The entire pPb data set is divided into classes based on the reconstructed track multiplicity, $N_{\text{trk}}^{\text{offline}}$, where primary tracks with $|\eta| < 2.4$ and $p_T > 0.4$ GeV are counted. Details of the multiplicity classification in this analysis, including the fraction of the full multiplicity distribution and the average number of primary tracks before and after correcting for detector effects in

each multiplicity range, are provided in Ref. [47].

A subset of semi-peripheral PbPb data collected during the 2011 LHC heavy-ion run with a minimum bias trigger are also reanalyzed in order to directly compare pPb and PbPb systems at the same collision multiplicity. The reanalyzed events were in the range of 50–100% centrality, where centrality is defined as the fraction of the total inelastic cross section, with 0% denoting the most central collisions. This sample was reprocessed using the same event selection and track reconstruction algorithm as for the present pPb analysis. A description of the 2011 PbPb data can be found in Refs. [47, 51].

4 Reconstruction of K_S^0 and $\Lambda/\bar{\Lambda}$ candidates

The reconstruction technique for K_S^0 and $\Lambda/\bar{\Lambda}$ candidates (generally referred to as V^0 s) at CMS was first described in Ref. [52]. To increase the efficiency for tracks with low momentum and large impact parameters, both characteristic of the K_S^0 and $\Lambda/\bar{\Lambda}$ decay products, the standard *loose* selection of tracks (as defined in Ref. [48]) is used in reconstructing the K_S^0 and $\Lambda/\bar{\Lambda}$ candidates. Oppositely charged tracks with at least 4 hits and both transverse and longitudinal impact parameter significances greater than 1 (with respect to the primary vertex) are first selected to form a secondary vertex. The distance of closest approach of the pair of tracks is required to be less than 0.5 cm. The fitted vertex in x, y, z of each pair of tracks is required to have a χ^2 value normalized by the number of degrees of freedom less than 7. The pair of tracks is assumed to be $\pi^+\pi^-$ in K_S^0 reconstruction, while the assumption of $\pi^-p(\pi^+\bar{p})$ is used in Λ ($\bar{\Lambda}$) reconstruction. For $\Lambda/\bar{\Lambda}$, the lower-momentum track is assumed to be the pion.

Due to the long lifetime of K_S^0 and $\Lambda/\bar{\Lambda}$ particles, a requirement on the significance of the V^0 decay length, which is the three-dimensional distance between the primary and V^0 vertices divided by its uncertainty, to be greater than 5 is applied to reduce background contributions. To remove K_S^0 candidates misidentified as $\Lambda/\bar{\Lambda}$ particles and vice versa, the $\Lambda/\bar{\Lambda}$ (K_S^0) candidates must have a corresponding $\pi^+\pi^-$ ($p\pi^-$) mass more than 20 (10) MeV away from the PDG value of the K_S^0 (Λ) mass [53]. The angle θ^{point} between the V^0 momentum vector and the vector connecting the primary and V^0 vertices is required to satisfy $\cos \theta^{\text{point}} > 0.999$. This reduces the effect of nuclear interactions, random combinations of tracks, and $\Lambda/\bar{\Lambda}$ particles originating from weak decays of Ξ and Ω^- particles. From MC simulations using GEANT4 and the HIJING event generator, it is found that the contribution of $\Lambda/\bar{\Lambda}$ particles from weak decays is less than 3% after this requirement. The K_S^0 ($\Lambda/\bar{\Lambda}$) reconstruction efficiency is about 6% (1%) for $p_T \approx 1$ GeV and 20% (10%) for $p_T > 3$ GeV within $|\eta| < 2.4$. This efficiency includes the effects of acceptance and the branching ratio for V^0 particle decays into neutral particles. The relatively low reconstruction efficiency of the V^0 candidates is primarily due to the decay length cut and the low efficiency for reconstructing daughter tracks with $p_T < 0.3$ GeV or large impact parameters.

Examples of invariant mass distributions of reconstructed K_S^0 and $\Lambda/\bar{\Lambda}$ candidates are shown in Fig. 1 for pPb data, with V^0 p_T in the range of 1–3 GeV and event multiplicity in the range $220 \leq N_{\text{trk}}^{\text{offline}} < 260$. Since the results for Λ and $\bar{\Lambda}$ are found to be consistent, they have been combined in this analysis. The V^0 peaks can be clearly identified with little background. The true V^0 signal peak is well described by a double Gaussian function (with a common mean), while the background is modeled by a 4th-order polynomial function fit over the entire mass range shown in Fig. 1. The mass window of $\pm 2\sigma$ wide around the center of the peak is defined as the “peak region”, where σ represents the root mean square of the two standard deviations of the double Gaussian functions weighted by the yields (with typical value of σ

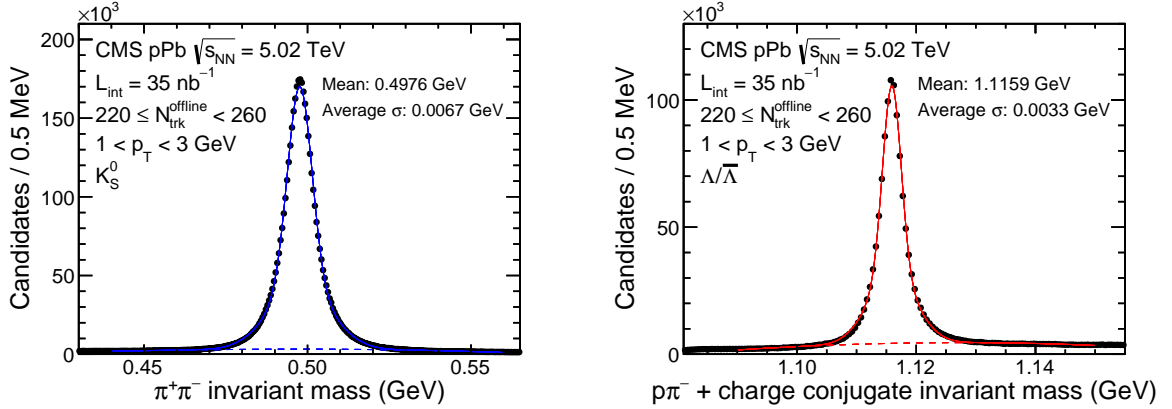


Figure 1: Invariant mass distribution of K_S^0 (left) and $\Lambda/\bar{\Lambda}$ (right) candidates in the p_T range of $1-3$ GeV for $220 \leq N_{\text{trk}}^{\text{offline}} < 260$ in pPb collisions at $\sqrt{s_{NN}} = 5.02$ TeV. The solid line shows the fit function of a double Gaussian plus a 4th-order polynomial (dashed line).

indicated in Fig. 1). To estimate the contribution of background candidates in the peak region to the correlation measurement, a “sideband region” is chosen that includes V^0 candidates from outside the $\pm 3\sigma$ mass range around the V^0 mass to the limit of the mass distributions shown in Fig. 1.

5 Analysis of two-particle correlations

The construction of the two-particle correlation function follows the same procedure established in Refs. [6, 7, 14, 47]. However, in this paper, reconstructed V^0 candidates from either the peak or sideband region are taken as “trigger” particles within a given p_T^{trig} range, instead of charged tracks as used in previous publications. The number of trigger V^0 candidates in the event is denoted by N_{trig} . Particle pairs are formed by associating each trigger particle with the remaining charged primary tracks in a specified p_T^{assoc} interval (which can be either the same as or different from the p_T^{trig} range). The two-dimensional (2D) correlation function is defined in the same way as in previous analyses as

$$\frac{1}{N_{\text{trig}}} \frac{d^2 N^{\text{pair}}}{d\Delta\eta \, d\Delta\phi} = B(0,0) \times \frac{S(\Delta\eta, \Delta\phi)}{B(\Delta\eta, \Delta\phi)}, \quad (1)$$

where $\Delta\eta$ and $\Delta\phi$ are the differences in η and ϕ of the pair. The same-event pair distribution, $S(\Delta\eta, \Delta\phi)$, represents the yield of particle pairs normalized by N_{trig} from the same event,

$$S(\Delta\eta, \Delta\phi) = \frac{1}{N_{\text{trig}}} \frac{d^2 N^{\text{same}}}{d\Delta\eta \, d\Delta\phi}. \quad (2)$$

The mixed-event pair distribution,

$$B(\Delta\eta, \Delta\phi) = \frac{1}{N_{\text{trig}}} \frac{d^2 N^{\text{mix}}}{d\Delta\eta \, d\Delta\phi}, \quad (3)$$

is constructed by pairing the trigger V^0 candidates in each event with the associated charged primary tracks from 20 different randomly selected events in the same 2 cm wide range of vertex position in the z direction and from the same track multiplicity class. Here, N^{mix} denotes the number of pairs taken from the mixed events. The ratio $B(0,0)/B(\Delta\eta, \Delta\phi)$ mainly accounts

for the pair acceptance effects, with $B(0, 0)$ representing the mixed-event associated yield for both particles of the pair going in approximately the same direction and thus having maximum pair acceptance (with a bin width of 0.3 in $\Delta\eta$ and $\pi/16$ in $\Delta\phi$). Thus, the quantity in Eq. (1) is effectively the per-trigger-particle associated yield. A pair is removed if the associated particle belongs to a daughter track of any trigger V^0 candidate (this contribution is negligible since associated particles are mostly primary tracks).

The same-event and mixed-event pair distributions are first calculated for each event, and then averaged over all the events within the track multiplicity class. The range of $0 < |\Delta\eta| < 4.8$ and $0 < |\Delta\phi| < \pi$ is used to fill one quadrant of the $(\Delta\eta, \Delta\phi)$ histograms, with the other three quadrants filled (for illustration purposes) by reflection to cover a $(\Delta\eta, \Delta\phi)$ range of $-4.8 < \Delta\eta < 4.8$ and $-\pi/2 < \Delta\phi < 3\pi/2$ for the 2D correlation functions, as will be shown later in Fig. 2. In performing the correlation analyses, each reconstructed primary track and V^0 candidate is weighted by a correction factor, following the procedure described in Refs. [6, 7, 14, 47]. This correction is also applied in calculating N_{trig} . This factor accounts for detector effects including the reconstruction efficiency, the detector acceptance, and the fraction of misreconstructed tracks. This correction factor is found to have a negligible effect on the azimuthal anisotropy harmonics.

5.1 Extraction of v_n harmonics

Motivated by hydrodynamic models of long-range correlations in pPb collisions, azimuthal anisotropy harmonics of K_S^0 and $\Lambda/\bar{\Lambda}$ particles are extracted via a Fourier decomposition of $\Delta\phi$ correlation functions averaged over $|\Delta\eta| > 2$ (to remove short-range correlations such as jet fragmentation),

$$\frac{1}{N_{\text{trig}}} \frac{dN^{\text{pair}}}{d\Delta\phi} = \frac{N_{\text{assoc}}}{2\pi} \left[1 + \sum_n 2V_{n\Delta} \cos(n\Delta\phi) \right], \quad (4)$$

as was done in Refs. [6, 7, 14, 47]. Here, $V_{n\Delta}$ are the Fourier coefficients and N_{assoc} represents the total number of pairs per trigger V^0 particle for a given $(p_T^{\text{trig}}, p_T^{\text{assoc}})$ bin. The first three Fourier terms are included in the fits to the correlation functions. Including additional terms has a negligible effect on the results of the Fourier fit.

If the observed two-particle azimuthal correlations arise purely as the result of convoluting anisotropic distributions of single particles, then the $V_{n\Delta}$ coefficients can be factorized into the product of single-particle anisotropies [47],

$$V_{n\Delta}(p_T^{\text{trig}}, p_T^{\text{assoc}}) = v_n(p_T^{\text{trig}}) \times v_n(p_T^{\text{assoc}}). \quad (5)$$

Following this assumption, the elliptic (v_2) and triangular (v_3) anisotropy harmonics of V^0 particles can be extracted as a function of p_T from the fitted Fourier coefficients,

$$v_n(p_T^{V^0}) = \frac{V_{n\Delta}(p_T^{V^0}, p_T^{\text{ref}})}{\sqrt{V_{n\Delta}(p_T^{\text{ref}}, p_T^{\text{ref}})}}, \quad n = 2, 3. \quad (6)$$

Here, a fixed p_T^{ref} range for the “reference” charged primary particles is chosen to be $0.3 < p_T < 3.0 \text{ GeV}$ (the lowest p_T region accessible by CMS and the same as was used in Ref. [47]), to minimize correlations from back-to-back jets at higher p_T .

The v_n values are first extracted for V^0 candidates from the peak region (which contains small contributions from background V^0 s) and sideband region, denoted as v_n^{obs} and v_n^{bkg} , respec-

tively. The v_n signal of true V^0 particles is denoted by v_n^{sig} and is obtained by

$$v_n^{\text{sig}} = \frac{v_n^{\text{obs}} - (1 - f^{\text{sig}}) \times v_n^{\text{bkg}}}{f^{\text{sig}}}, \quad n = 2, 3, \quad (7)$$

assuming v_n^{sig} and v_n^{bkg} are independent from each other. Here, f^{sig} represents the signal yield fraction in the peak region determined by the fits to the mass distribution shown in Fig. 1. This fraction exceeds 80% for $\Lambda/\bar{\Lambda}$ candidates at $p_T > 1 \text{ GeV}$ and is above 95% for K_S^0 candidates over the entire p_T range.

5.2 Systematic uncertainties

Table 1 summarizes different sources of systematic uncertainties in v_n^{sig} (identical for K_S^0 and $\Lambda/\bar{\Lambda}$ particles) for pPb and PbPb data. The dominant sources of systematic uncertainties are related to the reconstruction of V^0 candidates. The systematic effects are found to have no dependence on p_T so the estimated systematic uncertainties are assumed to be constant percentages over the entire p_T range. Systematic uncertainties in v_3^{sig} are assumed to be the same as those in v_2^{sig} , as was done in Ref. [47].

The range of the V^0 mass distributions used in fitting the signal plus background (Fig. 1) is varied by 10%. This change, which could affect the value of f^{sig} used in Eq. (7), yields a systematic uncertainty of less than 1% for the v_2^{sig} results. Changing the mass range included in the peak region could impact the values of both f^{sig} and v_2^{obs} . For a variation from $\pm 1\sigma$ to $\pm 3\sigma$, the v_2^{sig} values are found to be consistent within 2%. Systematic uncertainties due to selection of different sideband mass regions, which could change v_2^{bkg} , are estimated to be 2.2%. Possible contamination by residual misidentified V^0 candidates (i.e., K_S^0 as $\Lambda/\bar{\Lambda}$, and vice versa) is also investigated. Variation of the invariant mass range used to reject misidentified V^0 candidates leads to variations of less than 2% on v_2^{sig} . Systematic effects related to selection of the V^0 candidates are evaluated by varying the requirements on the decay length significance and $\cos \theta^{\text{point}}$, resulting in an uncertainty of 3%. As misalignment of the tracker detector elements can affect the V^0 reconstruction performance, an alternative detector geometry is studied. Compared to the standard configuration, this alternative has the two halves of the barrel pixel detector shifted in opposite directions along the beam by a distance on the order of 100 μm . The values of v_2^{sig} found using the shifted configuration differed by less than 2% from the default ones.

To test the procedure of extracting the V^0 signal v_2 from Eq. (7), a study using EPOS LHC pPb MC events is performed to compare the extracted v_2^{sig} results with the generator-level K_S^0 and $\Lambda/\bar{\Lambda}$ values. The agreement is found to be better than 4%. Other systematic uncertainties introduced by the high-multiplicity trigger efficiency (1%) and possible residual pile-up effects (1–2%) for pPb data are estimated in the same way as in Ref. [47], and found to make only a small contribution. The various sources of systematic uncertainties are added together in quadrature to arrive at the final systematic uncertainties (6.9% for pPb and 6.6% for PbPb), which are shown as shaded boxes in Figs. 4–7.

6 Results

The 2D two-particle correlation functions measured in pPb collisions for pairs of a K_S^0 (left) and $\Lambda/\bar{\Lambda}$ (right) trigger particles and a charged associated particle (h^\pm) are shown in Fig. 2 in the p_T range of 1–3 GeV. The 2D correlation functions are corrected for the background V^0

Table 1: Summary of systematic uncertainties in v_n^{sig} for pPb and PbPb data.

Source	pPb (%)	PbPb(%)
V^0 mass distribution range used in fit	1	1
Size of V^0 mass region for signal	2	2
Size and location of V^0 mass sideband region	2.2	2.2
Misidentified V^0 mass region	2	2
V^0 selection criteria	3	3
Tracker misalignment	2	2
MC closure test	4	4
Trigger efficiency	2	—
Pile-up	1	—
Total	6.9	6.6

candidates, following the same approach of correcting v_n in Eq. (7). The correction is negligible in this p_T range because of the high signal yield fraction of V^0 candidates. For low-multiplicity events ($N_{\text{trk}}^{\text{offline}} < 35$, Figs. 2 (a) and (b)), a sharp peak near $(\Delta\eta, \Delta\phi) = (0, 0)$ due to jet fragmentation (truncated for better illustration of the full correlation structure) can be clearly observed for both $K_S^0-h^\pm$ and $\Lambda/\bar{\Lambda}-h^\pm$ correlations. Moving to high-multiplicity events ($220 \leq N_{\text{trk}}^{\text{offline}} < 260$, Figs. 2 (c) and (d)), in addition to the peak from jet fragmentation, a pronounced long-range structure is seen at $\Delta\phi \approx 0$, extending at least 4.8 units in $|\Delta\eta|$. This structure was previously observed in high-multiplicity ($N_{\text{trk}}^{\text{offline}} \sim 110$) pp collisions at $\sqrt{s} = 7$ TeV [13] and pPb collisions at $\sqrt{s_{\text{NN}}} = 5.02$ TeV [14–16, 47] for inclusive charged particles, and also for identified charged pions, kaons, and protons in pPb collisions at $\sqrt{s_{\text{NN}}} = 5.02$ TeV [31]. A similar long-range correlation structure has also been extensively studied in AA collisions over a wide range of energies [1–9], where it is believed to arise primarily from collective flow of a strongly interacting medium [34].

To investigate the correlation structure for different species of particles in detail, one-dimensional (1D) distributions in $\Delta\phi$ are found by averaging the signal and mixed-event 2D distributions over $|\Delta\eta| < 1$ (defined as the “short-range region”) and $|\Delta\eta| > 2$ (defined as the “long-range region”), as done in Refs. [6, 7, 13, 14, 47]. Fig. 3 shows the 1D $\Delta\phi$ correlation functions from pPb data for trigger particles composed of inclusive charged particles (left) [47], K_S^0 particles (middle), and $\Lambda/\bar{\Lambda}$ particles (right), in the multiplicity range $N_{\text{trk}}^{\text{offline}} < 35$ (open) and $220 \leq N_{\text{trk}}^{\text{offline}} < 260$ (filled). The curves show the Fourier fits from Eq. (4) to the long-range region, which will be discussed in detail later. Following the standard zero-yield-at-minimum (ZYAM) procedure [47], each distribution is shifted to have zero associated yield at its minimum to represent the correlated portion of the associated yield. Selection of fixed p_T^{trig} and p_T^{assoc} ranges of 1–3 GeV is shown for the long-range region (top) and for the difference of the short- and long-range regions (bottom) in Fig. 3. As illustrated in Fig. 2, the near-side long-range signal remains nearly constant in $\Delta\eta$. Therefore, by taking a difference of 1D $\Delta\phi$ projections between the short- and long-range regions, the near-side jet correlations can be extracted. As shown in the bottom panels of Fig. 3, due to biases in multiplicity selection toward higher p_T jets, a larger jet peak yield is observed for events selected with higher multiplicities. Because charged particles are directly used in determining the multiplicity in the event, this selection bias is much stronger for charged particles than K_S^0 and $\Lambda/\bar{\Lambda}$ hadrons. For $N_{\text{trk}}^{\text{offline}} < 35$, no near-side correlations are observed in the long-range region for any particle species. The PbPb data show qualitatively the same behavior as the pPb data, and thus are not presented here.

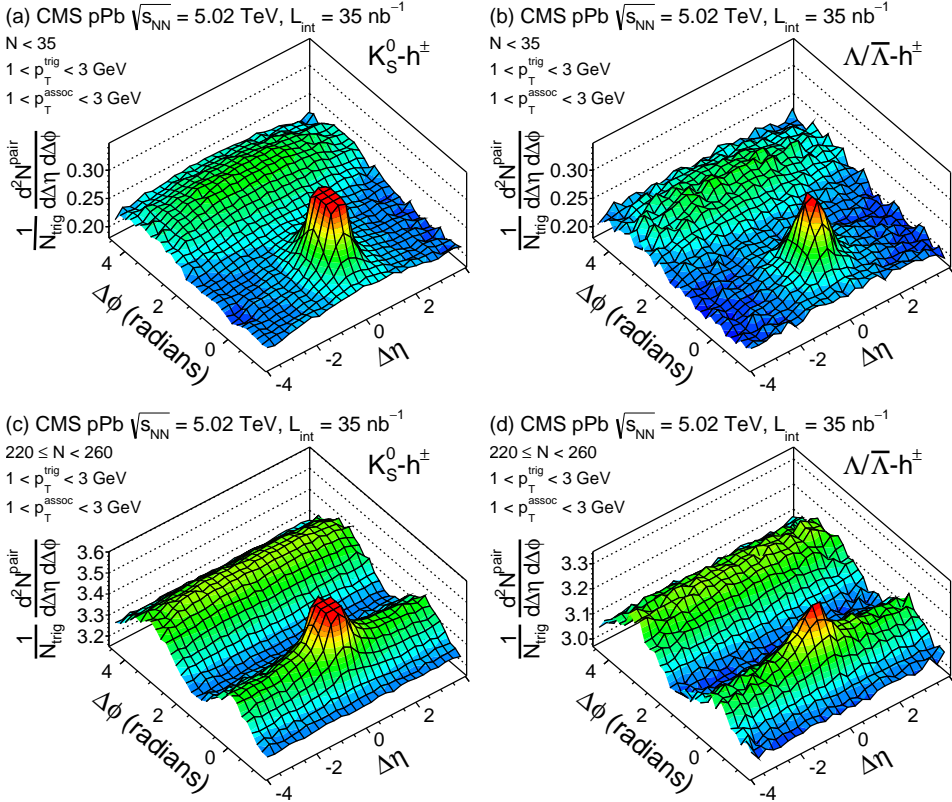


Figure 2: The 2D two-particle correlation functions in pPb collisions at $\sqrt{s_{NN}} = 5.02 \text{ TeV}$ for pairs of a K_S^0 (a,c) or $\Lambda/\bar{\Lambda}$ (b,d) trigger particle and a charged associated particle (h^\pm), with $1 < p_T^{\text{trig}} < 3 \text{ GeV}$ and $1 < p_T^{\text{assoc}} < 3 \text{ GeV}$, in the multiplicity ranges $N_{\text{trk}}^{\text{offline}} < 35$ (a, b) and $220 \leq N_{\text{trk}}^{\text{offline}} < 260$ (c, d). The sharp near-side peak from jet correlations is truncated to emphasize the structure outside that region.

Recently, the v_2 anisotropy harmonics for charged pions, kaons, and protons have been studied using two-particle correlations in pPb collisions [31], and are found to be qualitatively consistent with hydrodynamic models [32, 33]. In this paper, the elliptic (v_2) and triangular (v_3) flow harmonics of K_S^0 and $\Lambda/\bar{\Lambda}$ particles are extracted from the Fourier decomposition of 1D $\Delta\phi$ correlation functions for the long-range region ($|\Delta\eta| > 2$) in a significantly larger sample of pPb collisions such that the particle species dependence of v_n can be investigated in detail. In Fig. 4, the v_2^{sig} of K_S^0 and $\Lambda/\bar{\Lambda}$ particles are plotted as a function of p_T for the three lowest multiplicity ranges in PbPb and pPb collisions. These data were recorded using a minimum bias trigger. The range of the fraction of the full multiplicity distribution that each multiplicity selection corresponds to, as determined in Ref. [47], is also specified in the figure. In contrast to most other PbPb analyses, the present work uses multiplicity to classify events, instead of the total energy deposited in HF (the standard procedure of centrality determination in PbPb) [47, 51]. By examining the HF energy distribution for PbPb events in each of the multiplicity ranges, the corresponding average HF fractional cross section (and its standard deviation) can be determined, which are presented for PbPb data in the figure.

In the low multiplicity region (Fig. 4), the v_2 values of K_S^0 and $\Lambda/\bar{\Lambda}$ particles are compatible within statistical uncertainties. As there is no evident long-range near-side correlation seen in these low-multiplicity events, the extracted v_2 most likely reflects back-to-back jet correlations on the away side. Away-side jet correlations typically appear as a peak structure around $\Delta\phi \approx$

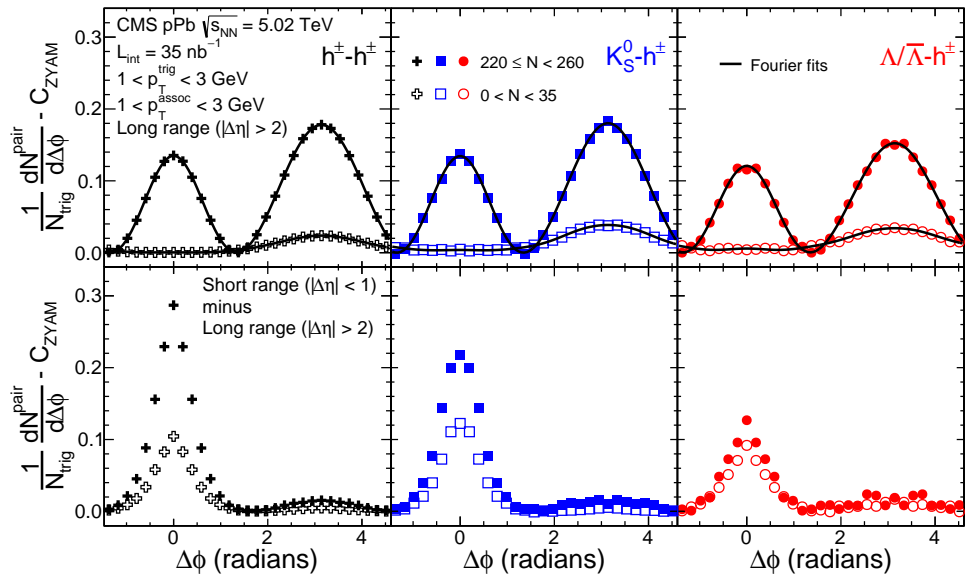


Figure 3: The 1D $\Delta\phi$ correlation functions from pPb data after applying the ZYAM procedure, in the multiplicity range $N_{\text{trk}}^{\text{offline}} < 35$ (open) and $220 \leq N_{\text{trk}}^{\text{offline}} < 260$ (filled), for trigger particles composed of inclusive charged particles (left), K_S^0 particles (middle), and $\Lambda/\bar{\Lambda}$ particles (right). Selection of a fixed p_T^{trig} and p_T^{assoc} range of both 1–3 GeV is shown for the long-range region ($|\Delta\eta| > 2$) on top and the short-range ($|\Delta\eta| < 1$) minus long-range region on the bottom. The curves on the top panels correspond to the Fourier fits including the first three terms. Statistical uncertainties are smaller than the size of the markers.

π , which contributes to various orders of Fourier terms.

The top row of Fig. 5 shows the measured v_2 values for K_S^0 and $\Lambda/\bar{\Lambda}$ particles as a function of p_T from the high multiplicity pPb data, along with the previously published results for inclusive charged particles [47]. In the $p_T \lesssim 2 \text{ GeV}$ region for all high-multiplicity ranges, the v_2 values of K_S^0 particles are larger than those for $\Lambda/\bar{\Lambda}$ particles at each p_T value. Both of them are consistently below the v_2 values of inclusive charged particles. As most charged particles are pions, the data indicate that lighter particle species exhibit a stronger azimuthal anisotropy signal. This mass ordering behavior is consistent with expectations in hydrodynamic models and the observation in 0–20% centrality pPb collisions [31]. A similar trend was first observed in AA collisions at RHIC [28, 29]. At higher p_T , the v_2 values of $\Lambda/\bar{\Lambda}$ particles are larger than those of K_S^0 . The inclusive charged particle v_2 values fall between the values of the two identified strange hadron species but are much closer to the v_2 values for K_S^0 particles. Note that the ratio of baryon to meson yield in pPb collisions is enhanced at higher p_T , an effect that becomes stronger as multiplicity increases [54, 55]. This should also be taken into account when comparing v_n values between inclusive and identified particles. Comparing the results in Fig. 4 and Fig. 5, the dependence of v_2 on the particle species may already be emerging in the multiplicity range of $60 \leq N_{\text{trk}}^{\text{offline}} < 120$.

The scaling behavior of v_2 divided by the number of constituent quarks as a function of transverse kinetic energy per quark, KE_T/n_q , is investigated for high-multiplicity pPb events in the middle row of Fig. 5. After scaling by the number of quarks, the v_2 distributions for K_S^0 and $\Lambda/\bar{\Lambda}$ particles are found to be in agreement. The middle row of Fig. 5 also shows the result of fitting a polynomial function to the K_S^0 data. The bottom row of Fig. 5 shows the n_q -scaled v_2 results for K_S^0 and $\Lambda/\bar{\Lambda}$ particles divided by this polynomial function fit, indicating that the scaling is valid to better than 10% over most of the KE_T/n_q range, except for $KE_T/n_q < 0.2 \text{ GeV}$

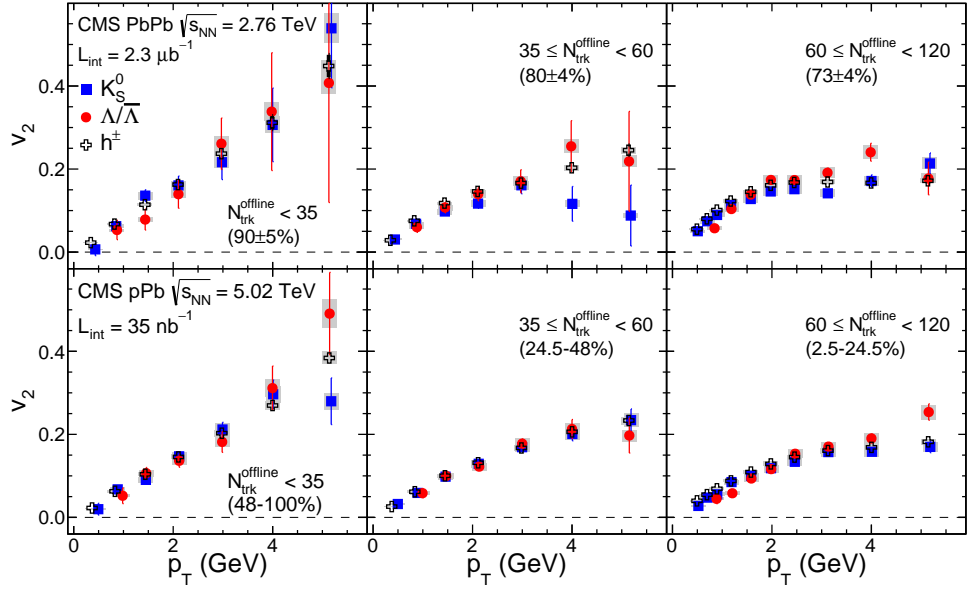


Figure 4: The v_2 results for K_S^0 (filled squares) and $\Lambda/\bar{\Lambda}$ (filled circles) particles as a function of p_T for three multiplicity ranges obtained from minimum bias triggered PbPb sample at $\sqrt{s_{NN}} = 2.76$ TeV (top row) and pPb sample at $\sqrt{s_{NN}} = 5.02$ TeV (bottom row). The error bars correspond to statistical uncertainties, while the shaded areas denote the systematic uncertainties. The values in parentheses give the mean and standard deviation of the HF fractional cross section for PbPb and the range of the fraction of the full multiplicity distribution included for pPb.

where the deviation grows to about 20%. In AA collisions, this approximate scaling behavior is conjectured to be related to quark recombination [39–41], which postulates that collective flow is developed among constituent quarks before they combine into final-state hadrons. Note that the scaling of v_2 with the number of constituent quarks was originally observed as a function of p_T , instead of KE_T , for the intermediate p_T range of a few GeV [38], and interpreted in a simple picture of quark coalescence [39]. However, it was later discovered that when plotted as a function of KE_T in order to remove the mass difference of identified hadrons, the scaling appears to hold over the entire kinematic range [42, 43]. However, this scaling behavior is not expected to be exact at low p_T in hydrodynamic models because of the impact of radial flow. As the v_n data tend to approach a constant value as a function of p_T or KE_T for $p_T \gtrsim 2$ GeV, the scaling behavior in terms of p_T and KE_T cannot be differentiated in that regime. Therefore, the n_q -scaled v_n results in this paper are presented as a function of KE_T/n_q in order to explore the scaling behavior over a wider kinematic range.

The particle species dependence of v_2 and its scaling behavior is also studied in PbPb data over the same multiplicity ranges as for the pPb data, as shown in Fig. 6. The mean and standard deviation of the HF fractional cross section of the PbPb data are indicated on the plots. Qualitatively, a similar particle-species dependence of v_2 is observed. However, the mass ordering effect is found to be less evident in PbPb data than in pPb data for all multiplicity ranges. In hydrodynamic models, this may indicate a stronger radial flow is developed in the pPb system as its energy density is higher than that of a PbPb system due to having a smaller size system at the same multiplicity. Moreover, the n_q -scaled v_2 data in PbPb at similar multiplicities suggest a stronger violation of constituent quark number scaling, up to 25%, than is observed in pPb, especially for higher KE_T/n_q values. This is also observed in peripheral AuAu collisions at RHIC, while the scaling applies more closely for central AuAu collisions [56].

The triangular flow harmonic, v_3 , of K_S^0 and $\Lambda/\bar{\Lambda}$ particles is also extracted in pPb and PbPb

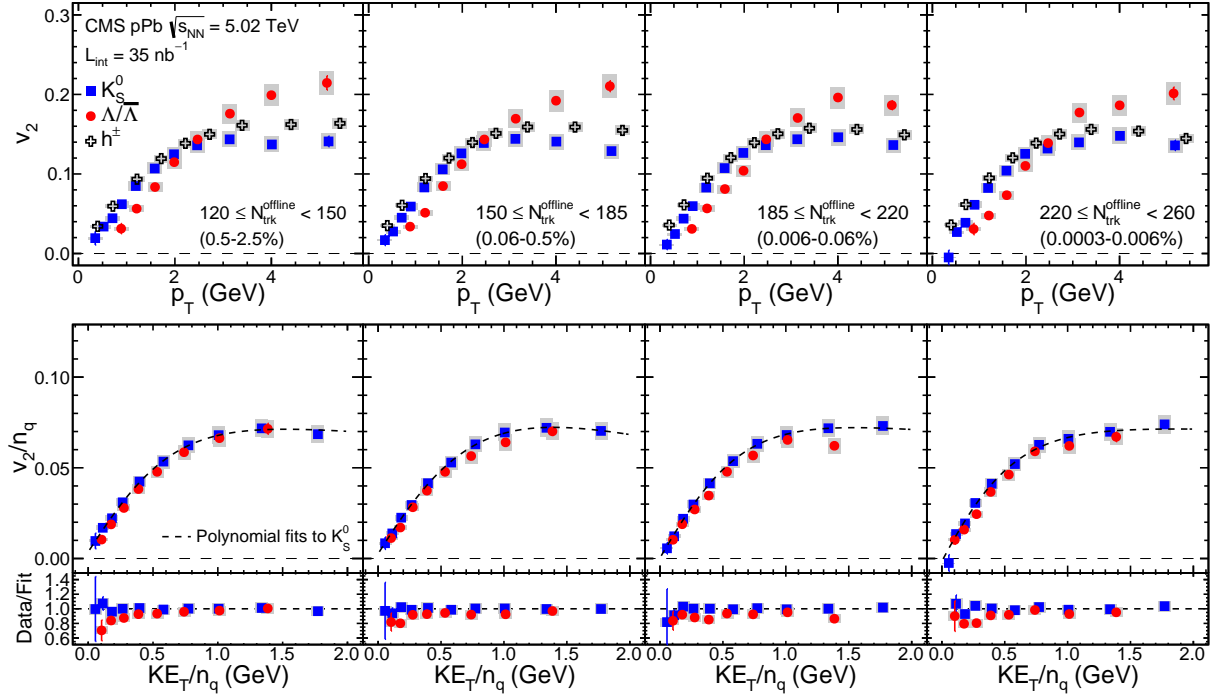


Figure 5: Top row: the v_2 results for K_S^0 (filled squares), $\Lambda/\bar{\Lambda}$ (filled circles), and inclusive charged particles (open crosses) as a function of p_T for four multiplicity ranges obtained from high-multiplicity triggered pPb sample at $\sqrt{s_{NN}} = 5.02$ TeV. Middle row: the v_2/n_q ratios for K_S^0 (filled squares) and $\Lambda/\bar{\Lambda}$ (filled circles) particles as a function of KE_T/n_q , along with a fit to the K_S^0 results using a polynomial function. Bottom row: ratios of v_2/n_q for K_S^0 and $\Lambda/\bar{\Lambda}$ particles to the fitted polynomial function as a function of KE_T/n_q . The error bars correspond to statistical uncertainties, while the shaded areas denote the systematic uncertainties. The values in parentheses give the range of the fraction of the full multiplicity distribution included for pPb.

collisions, as shown in Fig. 7. Due to limited statistical precision, only the result in the multiplicity range $185 \leq N_{\text{trk}}^{\text{offline}} < 350$ is presented. A similar species dependence of v_3 to that of v_2 is observed and, within the statistical uncertainties, the v_3 values scaled by the constituent quark number for K_S^0 and $\Lambda/\bar{\Lambda}$ particles match at the level of 20% over the full KE_T/n_q range. To date, no calculations of the quark number scaling of triangular flow, v_3 , have been performed in the parton recombination model.

7 Summary

Measurements of two-particle correlations with an identified K_S^0 or $\Lambda/\bar{\Lambda}$ trigger particle have been presented over a broad transverse momentum and pseudorapidity range in pPb collisions at $\sqrt{s_{NN}} = 5.02$ TeV and PbPb collisions at $\sqrt{s_{NN}} = 2.76$ TeV. With the implementation of a high-multiplicity trigger during the LHC 2013 pPb run, the identified particle correlation data in pPb collisions are explored over a broad particle multiplicity range, comparable to that covered by 50–100% centrality PbPb collisions. The long-range ($|\Delta\eta| > 2$) correlations are quantified in terms of azimuthal anisotropy Fourier harmonics (v_n) motivated by hydrodynamic models. In low-multiplicity pPb and PbPb events, similar v_2 values of K_S^0 and $\Lambda/\bar{\Lambda}$ particles are observed, which likely originate from back-to-back jet correlations. For higher event multiplicities, a particle species dependence of $v_2(p_T)$ and $v_3(p_T)$ is observed. For $p_T \lesssim 2$ GeV, the values

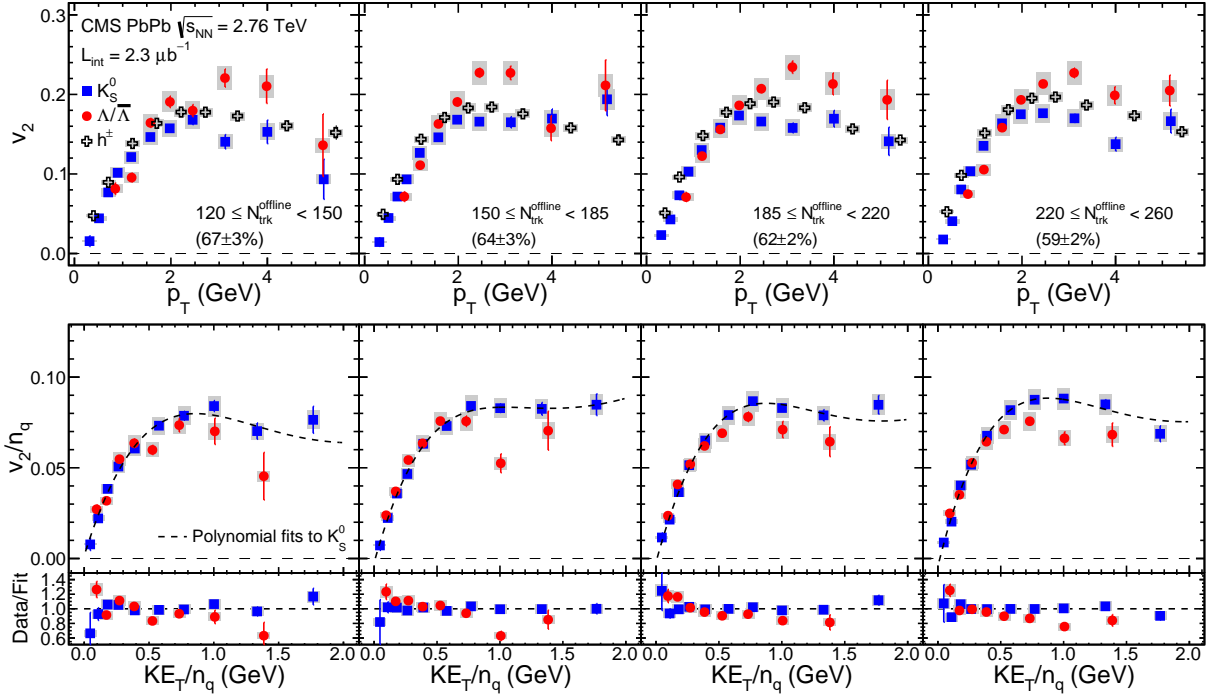


Figure 6: Top row: the v_2 results for K_S^0 (filled squares), $\Lambda/\bar{\Lambda}$ (filled circles), and inclusive charged particles (open crosses) as a function of p_T for four multiplicity ranges obtained from minimum bias triggered PbPb sample at $\sqrt{s_{NN}} = 2.76$ TeV. Middle row: the v_2/n_q ratios for K_S^0 (filled squares) and $\Lambda/\bar{\Lambda}$ (filled circles) particles as a function of KE_T/n_q . Bottom row: ratios of v_2/n_q for K_S^0 and $\Lambda/\bar{\Lambda}$ particles to a smooth fit function of v_2/n_q for K_S^0 particles as a function of KE_T/n_q . The error bars correspond to statistical uncertainties, while the shaded areas denote the systematic uncertainties. The values in parentheses give the mean and standard deviation of the HF fractional cross section for PbPb.

of v_n for K_S^0 particles are found to be larger than those of $\Lambda/\bar{\Lambda}$ particles, while this order is reversed at higher p_T . This behavior is consistent with RHIC and LHC results in AA collisions and for identified charged hadrons in pPb and dAu collisions. For similar event multiplicities, the particle species dependence of v_2 and v_3 at low p_T is observed to be more pronounced in pPb than in PbPb collisions. In the context of hydrodynamic models, this may indicate that a stronger radial flow boost is developed in pPb collisions. Furthermore, constituent quark number scaling of v_2 and v_3 between K_S^0 and $\Lambda/\bar{\Lambda}$ particles is found to apply for PbPb and high-multiplicity pPb events. The constituent quark number scaling is found to hold at the 10% (25%) level in pPb (PbPb) collisions, for similar event multiplicities. It will be interesting to see if this scaling law continues to hold for other particles. The results presented in this paper provide important input to the further exploration of the possible collective flow origin of long-range correlations, and can be used to evaluate models of quark recombination in a deconfined medium of quarks and gluons.

Acknowledgments

We congratulate our colleagues in the CERN accelerator departments for the excellent performance of the LHC and thank the technical and administrative staffs at CERN and at other CMS institutes for their contributions to the success of the CMS effort. In addition, we gratefully acknowledge the computing centres and personnel of the Worldwide LHC Computing Grid

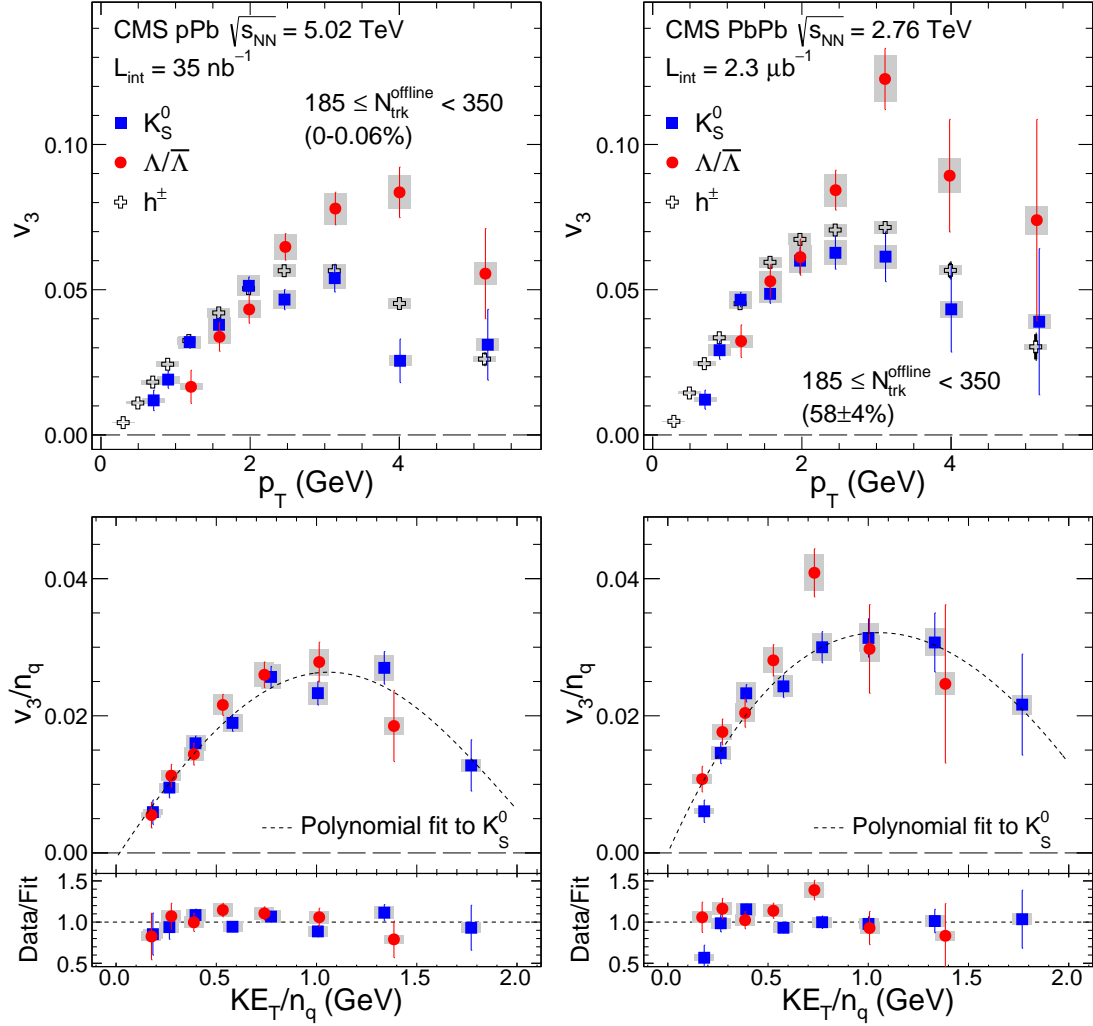


Figure 7: Top: the v_3 results for K_S^0 (filled squares), $\Lambda/\bar{\Lambda}$ (filled circles), and inclusive charged particles (open crosses) as a function of p_T for the multiplicity range $185 \leq N_{\text{trk}}^{\text{offline}} < 350$ in pPb collisions at $\sqrt{s_{NN}} = 5.02$ TeV (left) and in PbPb collisions at $\sqrt{s_{NN}} = 2.76$ TeV (right). Bottom: the n_q -scaled v_3 values of K_S^0 (filled squares) and $\Lambda/\bar{\Lambda}$ (filled circles) particles as a function of KE_T/n_q for the same two systems. Ratios of v_n/n_q to a smooth fit function of v_n/n_q for K_S^0 particles as a function of KE_T/n_q are also shown. The error bars correspond to statistical uncertainties, while the shaded areas denote the systematic uncertainties. The values in parentheses give the mean and standard deviation of the HF fractional cross section for PbPb and the range of the fraction of the full multiplicity distribution included for pPb.

for delivering so effectively the computing infrastructure essential to our analyses. Finally, we acknowledge the enduring support for the construction and operation of the LHC and the CMS detector provided by the following funding agencies: BMWFW and FWF (Austria); FNRS and FWO (Belgium); CNPq, CAPES, FAPERJ, and FAPESP (Brazil); MES (Bulgaria); CERN; CAS, MoST, and NSFC (China); COLCIENCIAS (Colombia); MSES and CSF (Croatia); RPF (Cyprus); MoER, ERC IUT and ERDF (Estonia); Academy of Finland, MEC, and HIP (Finland); CEA and CNRS/IN2P3 (France); BMBF, DFG, and HGF (Germany); GSRT (Greece); OTKA and NIH (Hungary); DAE and DST (India); IPM (Iran); SFI (Ireland); INFN (Italy); NRF and WCU (Republic of Korea); LAS (Lithuania); MOE and UM (Malaysia); CINVESTAV, CONACYT, SEP, and UASLP-FAI (Mexico); MBIE (New Zealand); PAEC (Pakistan); MSHE and NSC (Poland);

FCT (Portugal); JINR (Dubna); MON, RosAtom, RAS and RFBR (Russia); MESTD (Serbia); SEIDI and CPAN (Spain); Swiss Funding Agencies (Switzerland); MST (Taipei); ThEPCenter, IPST, STAR and NSTDA (Thailand); TUBITAK and TAEK (Turkey); NASU and SFFR (Ukraine); STFC (United Kingdom); DOE and NSF (USA).

Individuals have received support from the Marie-Curie programme and the European Research Council and EPLANET (European Union); the Leventis Foundation; the A. P. Sloan Foundation; the Alexander von Humboldt Foundation; the Belgian Federal Science Policy Office; the Fonds pour la Formation à la Recherche dans l'Industrie et dans l'Agriculture (FRIA-Belgium); the Agentschap voor Innovatie door Wetenschap en Technologie (IWT-Belgium); the Ministry of Education, Youth and Sports (MEYS) of the Czech Republic; the Council of Science and Industrial Research, India; the HOMING PLUS programme of Foundation for Polish Science, cofinanced from European Union, Regional Development Fund; the Compagnia di San Paolo (Torino); the Consorzio per la Fisica (Trieste); MIUR project 20108T4XTM (Italy); the Thalis and Aristeia programmes cofinanced by EU-ESF and the Greek NSRF; and the National Priorities Research Program by Qatar National Research Fund.

References

- [1] STAR Collaboration, “Distributions of charged hadrons associated with high transverse momentum particles in pp and Au + Au collisions at $\sqrt{s_{NN}} = 200 \text{ GeV}$ ”, *Phys. Rev. Lett.* **95** (2005) 152301, doi:10.1103/PhysRevLett.95.152301, arXiv:nucl-ex/0501016.
- [2] STAR Collaboration, “Long range rapidity correlations and jet production in high energy nuclear collisions”, *Phys. Rev. C* **80** (2009) 064912, doi:10.1103/PhysRevC.80.064912, arXiv:0909.0191.
- [3] PHOBOS Collaboration, “System size dependence of cluster properties from two-particle angular correlations in Cu+Cu and Au+Au collisions at $\sqrt{s_{NN}} = 200 \text{ GeV}$ ”, *Phys. Rev. C* **81** (2010) 024904, doi:10.1103/PhysRevC.81.024904, arXiv:0812.1172.
- [4] PHOBOS Collaboration, “High transverse momentum triggered correlations over a large pseudorapidity acceptance in Au+Au collisions at $\sqrt{s_{NN}} = 200 \text{ GeV}$ ”, *Phys. Rev. Lett.* **104** (2010) 062301, doi:10.1103/PhysRevLett.104.062301, arXiv:0903.2811.
- [5] STAR Collaboration, “Three-particle coincidence of the long range pseudorapidity correlation in high energy nucleus-nucleus collisions”, *Phys. Rev. Lett.* **105** (2010) 022301, doi:10.1103/PhysRevLett.105.022301, arXiv:0912.3977.
- [6] CMS Collaboration, “Long-range and short-range dihadron angular correlations in central PbPb collisions at $\sqrt{s_{NN}} = 2.76 \text{ TeV}$ ”, *JHEP* **07** (2011) 076, doi:10.1007/JHEP07(2011)076, arXiv:1105.2438.
- [7] CMS Collaboration, “Centrality dependence of dihadron correlations and azimuthal anisotropy harmonics in PbPb collisions at $\sqrt{s_{NN}} = 2.76 \text{ TeV}$ ”, *Eur. Phys. J. C* **72** (2012) 2012, doi:10.1140/epjc/s10052-012-2012-3, arXiv:1201.3158.
- [8] ALICE Collaboration, “Harmonic decomposition of two-particle angular correlations in Pb-Pb collisions at $\sqrt{s_{NN}} = 2.76 \text{ TeV}$ ”, *Phys. Lett. B* **708** (2012) 249, doi:10.1016/j.physletb.2012.01.060, arXiv:1109.2501.

- [9] ATLAS Collaboration, “Measurement of the azimuthal anisotropy for charged particle production in $\sqrt{s_{NN}} = 2.76$ TeV lead-lead collisions with the ATLAS detector”, *Phys. Rev. C* **86** (2012) 014907, doi:10.1103/PhysRevC.86.014907, arXiv:1203.3087.
- [10] CMS Collaboration, “Studies of azimuthal dihadron correlations in ultra-central PbPb collisions at $\sqrt{s_{NN}} = 2.76$ TeV”, *JHEP* **02** (2014) 088, doi:10.1007/JHEP02(2014)088, arXiv:1312.1845.
- [11] J.-Y. Ollitrault, “Anisotropy as a signature of transverse collective flow”, *Phys. Rev. D* **46** (1992) 229, doi:10.1103/PhysRevD.46.229.
- [12] B. Alver and G. Roland, “Collision geometry fluctuations and triangular flow in heavy-ion collisions”, *Phys. Rev. C* **81** (2010) 054905, doi:10.1103/PhysRevC.81.054905, arXiv:1003.0194.
- [13] CMS Collaboration, “Observation of long-range near-side angular correlations in proton-proton collisions at the LHC”, *JHEP* **09** (2010) 091, doi:10.1007/JHEP09(2010)091, arXiv:1009.4122.
- [14] CMS Collaboration, “Observation of long-range near-side angular correlations in pPb collisions at the LHC”, *Phys. Lett. B* **718** (2013) 795, doi:10.1016/j.physletb.2012.11.025, arXiv:1210.5482.
- [15] ALICE Collaboration, “Long-range angular correlations on the near and away side in pPb collisions at $\sqrt{s_{NN}} = 5.02$ TeV”, *Phys. Lett. B* **719** (2013) 29, doi:10.1016/j.physletb.2013.01.012, arXiv:1212.2001.
- [16] ATLAS Collaboration, “Observation of associated near-side and away-side long-range correlations in $\sqrt{s_{NN}} = 5.02$ TeV proton-lead collisions with the ATLAS detector”, *Phys. Rev. Lett.* **110** (2013) 182302, doi:10.1103/PhysRevLett.110.182302, arXiv:1212.5198.
- [17] PHENIX Collaboration, “Measurement of long-range angular correlation and quadrupole anisotropy of pions and (anti)protons in central d+Au collisions at $\sqrt{s_{NN}} = 200$ GeV”, (2014). arXiv:1404.7461.
- [18] W. Li, “Observation of a ridge correlation structure in high multiplicity proton-proton collisions: A brief review”, *Mod. Phys. Lett. A* **27** (2012) 1230018, doi:10.1142/S0217732312300182, arXiv:1206.0148.
- [19] P. Bożek, “Collective flow in p-Pb and d-Pd collisions at TeV energies”, *Phys. Rev. C* **85** (2012) 014911, doi:10.1103/PhysRevC.85.014911, arXiv:1112.0915.
- [20] P. Bożek and W. Broniowski, “Correlations from hydrodynamic flow in pPb collisions”, *Phys. Lett. B* **718** (2013) 1557, doi:10.1016/j.physletb.2012.12.051, arXiv:1211.0845.
- [21] K. Dusling and R. Venugopalan, “Explanation of systematics of CMS p+Pb high multiplicity dihadron data at $\sqrt{s_{NN}} = 5.02$ TeV”, *Phys. Rev. D* **87** (2013) 054014, doi:10.1103/PhysRevD.87.054014, arXiv:1211.3701.
- [22] K. Dusling and R. Venugopalan, “Evidence for BFKL and saturation dynamics from dihadron spectra at the LHC”, *Phys. Rev. D* **87** (2013) 051502, doi:10.1103/PhysRevD.87.051502, arXiv:1210.3890.

- [23] P. Huovinen et al., “Radial and elliptic flow at RHIC: further predictions”, *Phys. Lett. B* **503** (2001) 58, doi:10.1016/S0370-2693(01)00219-2, arXiv:hep-ph/0101136.
- [24] P. F. Kolb and U. W. Heinz, “Hydrodynamic description of ultrarelativistic heavy-ion collisions”, in *Quark gluon plasma 3*, R. C. Hwa and X. N. Wang, eds., p. 634. World Scientific, Singapore, 2003. arXiv:nucl-th/0305084.
- [25] C. Shen, U. Heinz, P. Huovinen, and H. Song, “Radial and elliptic flow in Pb+Pb collisions at energies available at the CERN Large Hadron Collider from viscous hydrodynamics”, *Phys. Rev. C* **84** (2011) 044903, doi:10.1103/PhysRevC.84.044903, arXiv:1105.3226.
- [26] STAR Collaboration, “Experimental and theoretical challenges in the search for the quark gluon plasma: The STAR Collaboration’s critical assessment of the evidence from RHIC collisions”, *Nucl. Phys. A* **757** (2005) 102, doi:10.1016/j.nuclphysa.2005.03.085, arXiv:nucl-ex/0501009.
- [27] PHENIX Collaboration, “Formation of dense partonic matter in relativistic nucleus-nucleus collisions at RHIC: Experimental evaluation by the PHENIX collaboration”, *Nucl. Phys. A* **757** (2005) 184, doi:10.1016/j.nuclphysa.2005.03.086, arXiv:nucl-ex/0410003.
- [28] PHENIX Collaboration, “Elliptic flow of identified hadrons in Au+Au collisions at $\sqrt{s_{NN}} = 200 \text{ GeV}$ ”, *Phys. Rev. Lett.* **91** (2003) 182301, doi:10.1103/PhysRevLett.91.182301, arXiv:nucl-ex/0305013.
- [29] STAR Collaboration, “Identified particle elliptic flow in Au + Au collisions at $\sqrt{s_{NN}} = 130 \text{ GeV}$ ”, *Phys. Rev. Lett.* **87** (2001) 182301, doi:10.1103/PhysRevLett.87.182301, arXiv:nucl-ex/0107003.
- [30] ALICE Collaboration, “Elliptic flow of identified hadrons in Pb-Pb collisions at $\sqrt{s_{NN}} = 2.76 \text{ TeV}$ ”, (2014). arXiv:1405.4632.
- [31] ALICE Collaboration, “Long-range angular correlations of π , K and p in p-Pb collisions at $\sqrt{s_{NN}} = 5.02 \text{ TeV}$ ”, *Phys. Lett. B* **726** (2013) 164, doi:10.1016/j.physletb.2013.08.024, arXiv:1307.3237.
- [32] K. Werner et al., “Evidence for flow from hydrodynamic simulations of pPb collisions at 5.02 TeV from v_2 mass splitting”, *Phys. Rev. Lett.* **112** (2014) 232301, doi:10.1103/PhysRevLett.112.232301, arXiv:1307.4379.
- [33] P. Bożek, W. Broniowski, and G. Torrieri, “Mass hierarchy in identified particle distributions in proton-lead collisions”, *Phys. Rev. Lett.* **111** (2013) 172303, doi:10.1103/PhysRevLett.111.172303, arXiv:1307.5060.
- [34] S. Voloshin and Y. Zhang, “Flow study in relativistic nuclear collisions by Fourier expansion of azimuthal particle distributions”, *Z. Phys. C* **70** (1996) 665, doi:10.1007/s002880050141, arXiv:hep-ph/9407282.
- [35] B. H. Alver, C. Gombeaud, M. Luzum, and J.-Y. Ollitrault, “Triangular flow in hydrodynamics and transport theory”, *Phys. Rev. C* **82** (2010) 034913, doi:10.1103/PhysRevC.82.034913, arXiv:1007.5469.

- [36] B. Schenke, S. Jeon, and C. Gale, “Elliptic and triangular flow in event-by-event D=3+1 viscous hydrodynamics”, *Phys. Rev. Lett.* **106** (2011) 042301, doi:10.1103/PhysRevLett.106.042301, arXiv:1009.3244.
- [37] Z. Qiu, C. Shen, and U. Heinz, “Hydrodynamic elliptic and triangular flow in Pb-Pb collisions at $\sqrt{s_{NN}} = 2.76A$ TeV”, *Phys. Lett. B* **707** (2012) 151, doi:10.1016/j.physletb.2011.12.041, arXiv:1110.3033.
- [38] STAR Collaboration, “Particle type dependence of azimuthal anisotropy and nuclear modification of particle production in Au + Au collisions at $\sqrt{s_{NN}} = 200$ GeV”, *Phys. Rev. Lett.* **92** (2004) 052302, doi:10.1103/PhysRevLett.92.052302, arXiv:nucl-ex/0306007.
- [39] D. Molnar and S. A. Voloshin, “Elliptic flow at large transverse momenta from quark coalescence”, *Phys. Rev. Lett.* **91** (2003) 092301, doi:10.1103/PhysRevLett.91.092301, arXiv:nucl-th/0302014.
- [40] V. Greco, C. M. Ko, and P. Levai, “Parton coalescence and the anti-proton / pion anomaly at RHIC”, *Phys. Rev. Lett.* **90** (2003) 202302, doi:10.1103/PhysRevLett.90.202302, arXiv:nucl-th/0301093.
- [41] R. J. Fries, B. Muller, C. Nonaka, and S. A. Bass, “Hadronization in heavy ion collisions: Recombination and fragmentation of partons”, *Phys. Rev. Lett.* **90** (2003) 202303, doi:10.1103/PhysRevLett.90.202303, arXiv:nucl-th/0301087.
- [42] STAR Collaboration, “Mass, quark-number, and $\sqrt{s_{NN}}$ dependence of the second and fourth flow harmonics in ultra-relativistic nucleus-nucleus collisions”, *Phys. Rev. C* **75** (2007) 054906, doi:10.1103/PhysRevC.75.054906, arXiv:nucl-ex/0701010.
- [43] PHENIX Collaboration, “Scaling properties of azimuthal anisotropy in Au+Au and Cu+Cu collisions at $\sqrt{s_{NN}} = 200$ GeV”, *Phys. Rev. Lett.* **98** (2007) 162301, doi:10.1103/PhysRevLett.98.162301, arXiv:nucl-ex/0608033.
- [44] CMS Collaboration, “The CMS experiment at the CERN LHC”, *JINST* **3** (2008) S08004, doi:10.1088/1748-0221/3/08/S08004.
- [45] Geant4 Collaboration, “Geant4—a simulation toolkit”, *Nucl. Instrum. Meth. A* **506** (2003) 250, doi:10.1016/S0168-9002(03)01368-8.
- [46] CMS Collaboration, “Luminosity calibration for the 2013 proton-lead and proton-proton data taking”, CMS Physics Analysis Summary CMS-PAS-LUM-13-002, (2014).
- [47] CMS Collaboration, “Multiplicity and transverse momentum dependence of two- and four-particle correlations in pPb and PbPb collisions”, *Phys. Lett. B* **724** (2013) 213, doi:10.1016/j.physletb.2013.06.028, arXiv:1305.0609.
- [48] CMS Collaboration, “Description and performance of track and primary-vertex reconstruction with the CMS tracker”, (2014). arXiv:1405.6569.
- [49] T. Pierog et al., “EPOS LHC : test of collective hadronization with LHC data”, (2013). arXiv:1306.0121.
- [50] M. Gyulassy and X.-N. Wang, “HIJING 1.0: A Monte Carlo program for parton and particle production in high-energy hadronic and nuclear collisions”, *Comput. Phys. Commun.* **83** (1994) 307, doi:10.1016/0010-4655(94)90057-4, arXiv:nucl-th/9502021.

- [51] CMS Collaboration, "Azimuthal anisotropy of charged particles at high transverse momenta in PbPb collisions at $\sqrt{s_{NN}} = 2.76 \text{ TeV}$ ", *Phys. Rev. Lett.* **109** (2012) 022301, doi:10.1103/PhysRevLett.109.022301, arXiv:1204.1850.
- [52] CMS Collaboration, "Strange particle production in pp collisions at $\sqrt{s} = 0.9$ and 7 TeV ", *JHEP* **05** (2011) 064, doi:10.1007/JHEP05(2011)064, arXiv:1102.4282.
- [53] Particle Data Group Collaboration, "Review of Particle Physics (RPP)", *Phys. Rev. D* **86** (2012) 010001, doi:10.1103/PhysRevD.86.010001.
- [54] CMS Collaboration, "Study of the production of charged pions, kaons, and protons in pPb collisions at $\sqrt{s_{NN}} = 5.02 \text{ TeV}$ ", *Eur. Phys. J. C* **72** (2013) 2012, doi:10.1140/epjc/s10052-014-2847-x, arXiv:1307.3442.
- [55] ALICE Collaboration, "Multiplicity dependence of pion, kaon, proton and Lambda production in p-Pb collisions at $\sqrt{s_{NN}} = 5.02 \text{ TeV}$ ", *Phys. Lett. B* **728** (2014) 25, doi:10.1016/j.physletb.2013.11.020, arXiv:1307.6796.
- [56] PHENIX Collaboration, "Deviation from quark-number scaling of the anisotropy parameter v_2 of pions, kaons, and protons in Au+Au collisions at $\sqrt{s_{NN}} = 200 \text{ GeV}$ ", *Phys. Rev. C* **85** (2012) 064914, doi:10.1103/PhysRevC.85.064914, arXiv:1203.2644.

A The CMS Collaboration

Yerevan Physics Institute, Yerevan, Armenia
V. Khachatryan, A.M. Sirunyan, A. Tumasyan

Institut für Hochenergiephysik der OeAW, Wien, Austria

W. Adam, T. Bergauer, M. Dragicevic, J. Erö, C. Fabjan¹, M. Friedl, R. Frühwirth¹, V.M. Ghete,
C. Hartl, N. Hörmann, J. Hrubec, M. Jeitler¹, W. Kiesenhofer, V. Knünz, M. Krammer¹,
I. Krätschmer, D. Liko, I. Mikulec, D. Rabady², B. Rahbaran, H. Rohringer, R. Schöfbeck,
J. Strauss, A. Taurok, W. Treberer-Treberspurg, W. Waltenberger, C.-E. Wulz¹

National Centre for Particle and High Energy Physics, Minsk, Belarus

V. Mossolov, N. Shumeiko, J. Suarez Gonzalez

Universiteit Antwerpen, Antwerpen, Belgium

S. Alderweireldt, M. Bansal, S. Bansal, T. Cornelis, E.A. De Wolf, X. Janssen, A. Knutsson,
S. Luyckx, S. Ochesanu, R. Rougny, M. Van De Klundert, H. Van Haevermaet, P. Van Mechelen,
N. Van Remortel, A. Van Spilbeeck

Vrije Universiteit Brussel, Brussel, Belgium

F. Blekman, S. Blyweert, J. D'Hondt, N. Daci, N. Heracleous, J. Keaveney, S. Lowette, M. Maes,
A. Olbrechts, Q. Python, D. Strom, S. Tavernier, W. Van Doninck, P. Van Mulders, G.P. Van
Onsem, I. Villella

Université Libre de Bruxelles, Bruxelles, Belgium

C. Caillol, B. Clerbaux, G. De Lentdecker, D. Dobur, L. Favart, A.P.R. Gay, A. Grebenyuk,
A. Léonard, A. Mohammadi, L. Perniè², T. Reis, T. Seva, L. Thomas, C. Vander Velde, P. Vanlaer,
J. Wang, F. Zenoni

Ghent University, Ghent, Belgium

V. Adler, K. Beernaert, L. Benucci, A. Cimmino, S. Costantini, S. Crucy, S. Dildick, A. Fagot,
G. Garcia, J. Mccartin, A.A. Ocampo Rios, D. Ryckbosch, S. Salva Diblen, M. Sigamani,
N. Strobbe, F. Thyssen, M. Tytgat, E. Yazgan, N. Zaganidis

Université Catholique de Louvain, Louvain-la-Neuve, Belgium

S. Basegmez, C. Beluffi³, G. Bruno, R. Castello, A. Caudron, L. Ceard, G.G. Da Silveira,
C. Delaere, T. du Pree, D. Favart, L. Forthomme, A. Giannanco⁴, J. Hollar, A. Jafari, P. Jez,
M. Komm, V. Lemaitre, C. Nuttens, D. Pagano, L. Perrini, A. Pin, K. Piotrzkowski, A. Popov⁵,
L. Quertenmont, M. Selvaggi, M. Vidal Marono, J.M. Vizan Garcia

Université de Mons, Mons, Belgium

N. Belyi, T. Caebergs, E. Daubie, G.H. Hammad

Centro Brasileiro de Pesquisas Fisicas, Rio de Janeiro, Brazil

W.L. Aldá Júnior, G.A. Alves, L. Brito, M. Correa Martins Junior, T. Dos Reis Martins, C. Mora
Herrera, M.E. Pol

Universidade do Estado do Rio de Janeiro, Rio de Janeiro, Brazil

W. Carvalho, J. Chinellato⁶, A. Custódio, E.M. Da Costa, D. De Jesus Damiao, C. De Oliveira
Martins, S. Fonseca De Souza, H. Malbouisson, D. Matos Figueiredo, L. Mundim, H. Nogima,
W.L. Prado Da Silva, J. Santaolalla, A. Santoro, A. Sznajder, E.J. Tonelli Manganote⁶, A. Vilela
Pereira

Universidade Estadual Paulista ^a, Universidade Federal do ABC ^b, São Paulo, Brazil
 C.A. Bernardes^b, S. Dogra^a, T.R. Fernandez Perez Tomei^a, E.M. Gregores^b, P.G. Mercadante^b,
 S.F. Novaes^a, Sandra S. Padula^a

Institute for Nuclear Research and Nuclear Energy, Sofia, Bulgaria

A. Aleksandrov, V. Genchev², P. Iaydjiev, A. Marinov, S. Piperov, M. Rodozov, S. Stoykova,
 G. Sultanov, V. Tcholakov, M. Vutova

University of Sofia, Sofia, Bulgaria

A. Dimitrov, I. Glushkov, R. Hadjiiska, V. Kozuharov, L. Litov, B. Pavlov, P. Petkov

Institute of High Energy Physics, Beijing, China

J.G. Bian, G.M. Chen, H.S. Chen, M. Chen, R. Du, C.H. Jiang, R. Plestina⁷, J. Tao, Z. Wang

State Key Laboratory of Nuclear Physics and Technology, Peking University, Beijing, China
 C. Asawatangtrakuldee, Y. Ban, S. Liu, Y. Mao, S.J. Qian, D. Wang, L. Zhang, W. Zou

Universidad de Los Andes, Bogota, Colombia

C. Avila, L.F. Chaparro Sierra, C. Florez, J.P. Gomez, B. Gomez Moreno, J.C. Sanabria

**University of Split, Faculty of Electrical Engineering, Mechanical Engineering and Naval
 Architecture, Split, Croatia**

N. Godinovic, D. Lelas, D. Polic, I. Puljak

University of Split, Faculty of Science, Split, Croatia

Z. Antunovic, M. Kovac

Institute Rudjer Boskovic, Zagreb, Croatia

V. Brigljevic, K. Kadija, J. Luetic, D. Mekterovic, L. Sudic

University of Cyprus, Nicosia, Cyprus

A. Attikis, G. Mavromanolakis, J. Mousa, C. Nicolaou, F. Ptochos, P.A. Razis

Charles University, Prague, Czech Republic

M. Bodlak, M. Finger, M. Finger Jr.⁸

**Academy of Scientific Research and Technology of the Arab Republic of Egypt, Egyptian
 Network of High Energy Physics, Cairo, Egypt**

Y. Assran⁹, A. Ellithi Kamel¹⁰, M.A. Mahmoud¹¹, A. Radi^{12,13}

National Institute of Chemical Physics and Biophysics, Tallinn, Estonia

M. Kadastik, M. Murumaa, M. Raidal, A. Tiko

Department of Physics, University of Helsinki, Helsinki, Finland

P. Eerola, G. Fedi, M. Voutilainen

Helsinki Institute of Physics, Helsinki, Finland

J. Hätkönen, V. Karimäki, R. Kinnunen, M.J. Kortelainen, T. Lampén, K. Lassila-Perini, S. Lehti,
 T. Lindén, P. Luukka, T. Mäenpää, T. Peltola, E. Tuominen, J. Tuominiemi, E. Tuovinen,
 L. Wendland

Lappeenranta University of Technology, Lappeenranta, Finland

J. Talvitie, T. Tuuva

DSM/IRFU, CEA/Saclay, Gif-sur-Yvette, France

M. Besancon, F. Couderc, M. Dejardin, D. Denegri, B. Fabbro, J.L. Faure, C. Favaro, F. Ferri,

S. Ganjour, A. Givernaud, P. Gras, G. Hamel de Monchenault, P. Jarry, E. Locci, J. Malcles, J. Rander, A. Rosowsky, M. Titov

Laboratoire Leprince-Ringuet, Ecole Polytechnique, IN2P3-CNRS, Palaiseau, France

S. Baffioni, F. Beaudette, P. Busson, C. Charlot, T. Dahms, M. Dalchenko, L. Dobrzynski, N. Filipovic, A. Florent, R. Granier de Cassagnac, L. Mastrolorenzo, P. Miné, C. Mironov, I.N. Naranjo, M. Nguyen, C. Ochando, P. Paganini, S. Regnard, R. Salerno, J.B. Sauvan, Y. Sirois, C. Veelken, Y. Yilmaz, A. Zabi

Institut Pluridisciplinaire Hubert Curien, Université de Strasbourg, Université de Haute Alsace Mulhouse, CNRS/IN2P3, Strasbourg, France

J.-L. Agram¹⁴, J. Andrea, A. Aubin, D. Bloch, J.-M. Brom, E.C. Chabert, C. Collard, E. Conte¹⁴, J.-C. Fontaine¹⁴, D. Gelé, U. Goerlach, C. Goetzmann, A.-C. Le Bihan, P. Van Hove

Centre de Calcul de l’Institut National de Physique Nucléaire et de Physique des Particules, CNRS/IN2P3, Villeurbanne, France

S. Gadrat

Université de Lyon, Université Claude Bernard Lyon 1, CNRS-IN2P3, Institut de Physique Nucléaire de Lyon, Villeurbanne, France

S. Beauceron, N. Beaupere, G. Boudoul², E. Bouvier, S. Brochet, C.A. Carrillo Montoya, J. Chasserat, R. Chierici, D. Contardo², P. Depasse, H. El Mamouni, J. Fan, J. Fay, S. Gascon, M. Gouzevitch, B. Ille, T. Kurca, M. Lethuillier, L. Mirabito, S. Perries, J.D. Ruiz Alvarez, D. Sabes, L. Sgandurra, V. Sordini, M. Vander Donckt, P. Verdier, S. Viret, H. Xiao

Institute of High Energy Physics and Informatization, Tbilisi State University, Tbilisi, Georgia

Z. Tsamalaidze⁸

RWTH Aachen University, I. Physikalisches Institut, Aachen, Germany

C. Autermann, S. Beranek, M. Bontenackels, M. Edelhoff, L. Feld, O. Hindrichs, K. Klein, A. Ostapchuk, A. Perieanu, F. Raupach, J. Sammet, S. Schael, H. Weber, B. Wittmer, V. Zhukov⁵

RWTH Aachen University, III. Physikalisches Institut A, Aachen, Germany

M. Ata, M. Brodski, E. Dietz-Laursonn, D. Duchardt, M. Erdmann, R. Fischer, A. Güth, T. Hebbeker, C. Heidemann, K. Hoepfner, D. Klingebiel, S. Knutzen, P. Kreuzer, M. Merschmeyer, A. Meyer, P. Millet, M. Olschewski, K. Padeken, P. Papacz, H. Reithler, S.A. Schmitz, L. Sonnenschein, D. Teyssier, S. Thüer, M. Weber

RWTH Aachen University, III. Physikalisches Institut B, Aachen, Germany

V. Cherepanov, Y. Erdogan, G. Flügge, H. Geenen, M. Geisler, W. Haj Ahmad, A. Heister, F. Hoehle, B. Kargoll, T. Kress, Y. Kuessel, A. Künsken, J. Lingemann², A. Nowack, I.M. Nugent, L. Perchalla, O. Pooth, A. Stahl

Deutsches Elektronen-Synchrotron, Hamburg, Germany

I. Asin, N. Bartosik, J. Behr, W. Behrenhoff, U. Behrens, A.J. Bell, M. Bergholz¹⁵, A. Bethani, K. Borras, A. Burgmeier, A. Cakir, L. Calligaris, A. Campbell, S. Choudhury, F. Costanza, C. Diez Pardos, S. Dooling, T. Dorland, G. Eckerlin, D. Eckstein, T. Eichhorn, G. Flucke, J. Garay Garcia, A. Geiser, P. Gunnellini, J. Hauk, M. Hempel¹⁵, D. Horton, H. Jung, A. Kalogeropoulos, M. Kasemann, P. Katsas, J. Kieseler, C. Kleinwort, D. Krücker, W. Lange, J. Leonard, K. Lipka, A. Lobanov, W. Lohmann¹⁵, B. Lutz, R. Mankel, I. Marfin¹⁵, I.-A. Melzer-Pellmann, A.B. Meyer, G. Mittag, J. Mnich, A. Mussgiller, S. Naumann-Emme, A. Nayak, O. Novgorodova, E. Ntomari, H. Perrey, D. Pitzl, R. Placakyte, A. Raspereza, P.M. Ribeiro Cipriano, B. Roland, E. Ron, M.Ö. Sahin, J. Salfeld-Nebgen, P. Saxena, R. Schmidt¹⁵,

T. Schoerner-Sadenius, M. Schröder, C. Seitz, S. Spannagel, A.D.R. Vargas Trevino, R. Walsh, C. Wissing

University of Hamburg, Hamburg, Germany

M. Aldaya Martin, V. Blobel, M. Centis Vignal, A.R. Draeger, J. Erfle, E. Garutti, K. Goebel, M. Görner, J. Haller, M. Hoffmann, R.S. Höing, H. Kirschenmann, R. Klanner, R. Kogler, J. Lange, T. Lapsien, T. Lenz, I. Marchesini, J. Ott, T. Peiffer, N. Pietsch, J. Poehlsen, T. Poehlsen, D. Rathjens, C. Sander, H. Schettler, P. Schleper, E. Schlieckau, A. Schmidt, M. Seidel, V. Sola, H. Stadie, G. Steinbrück, D. Troendle, E. Usai, L. Vanelderden, A. Vanhoefer

Institut für Experimentelle Kernphysik, Karlsruhe, Germany

C. Barth, C. Baus, J. Berger, C. Böser, E. Butz, T. Chwalek, W. De Boer, A. Descroix, A. Dierlamm, M. Feindt, F. Frensch, M. Giffels, F. Hartmann², T. Hauth², U. Husemann, I. Katkov⁵, A. Kornmayer², E. Kuznetsova, P. Lobelle Pardo, M.U. Mozer, Th. Müller, A. Nürnberg, G. Quast, K. Rabbertz, F. Ratnikov, S. Röcker, H.J. Simonis, F.M. Stober, R. Ulrich, J. Wagner-Kuhr, S. Wayand, T. Weiler, R. Wolf

Institute of Nuclear and Particle Physics (INPP), NCSR Demokritos, Aghia Paraskevi, Greece

G. Anagnostou, G. Daskalakis, T. Geralis, V.A. Giakoumopoulou, A. Kyriakis, D. Loukas, A. Markou, C. Markou, A. Psallidas, I. Topsis-Giotis

University of Athens, Athens, Greece

S. Kesisoglou, A. Panagiotou, N. Saoulidou, E. Stiliaris

University of Ioánnina, Ioánnina, Greece

X. Aslanoglou, I. Evangelou, G. Flouris, C. Foudas, P. Kokkas, N. Manthos, I. Papadopoulos, E. Paradas

Wigner Research Centre for Physics, Budapest, Hungary

G. Bencze, C. Hajdu, P. Hidas, D. Horvath¹⁶, F. Sikler, V. Veszpremi, G. Vesztregombi¹⁷, A.J. Zsigmond

Institute of Nuclear Research ATOMKI, Debrecen, Hungary

N. Beni, S. Czellar, J. Karancsi¹⁸, J. Molnar, J. Palinkas, Z. Szillasi

University of Debrecen, Debrecen, Hungary

P. Raics, Z.L. Trocsanyi, B. Ujvari

National Institute of Science Education and Research, Bhubaneswar, India

S.K. Swain

Panjab University, Chandigarh, India

S.B. Beri, V. Bhatnagar, R. Gupta, U.Bhawandep, A.K. Kalsi, M. Kaur, R. Kumar, M. Mittal, N. Nishu, J.B. Singh

University of Delhi, Delhi, India

Ashok Kumar, Arun Kumar, S. Ahuja, A. Bhardwaj, B.C. Choudhary, A. Kumar, S. Malhotra, M. Naimuddin, K. Ranjan, V. Sharma

Saha Institute of Nuclear Physics, Kolkata, India

S. Banerjee, S. Bhattacharya, K. Chatterjee, S. Dutta, B. Gomber, Sa. Jain, Sh. Jain, R. Khurana, A. Modak, S. Mukherjee, D. Roy, S. Sarkar, M. Sharan

Bhabha Atomic Research Centre, Mumbai, India

A. Abdulsalam, D. Dutta, S. Kailas, V. Kumar, A.K. Mohanty², L.M. Pant, P. Shukla, A. Topkar

Tata Institute of Fundamental Research, Mumbai, India

T. Aziz, S. Banerjee, S. Bhowmik¹⁹, R.M. Chatterjee, R.K. Dewanjee, S. Dugad, S. Ganguly, S. Ghosh, M. Guchait, A. Gurtu²⁰, G. Kole, S. Kumar, M. Maity¹⁹, G. Majumder, K. Mazumdar, G.B. Mohanty, B. Parida, K. Sudhakar, N. Wickramage²¹

Institute for Research in Fundamental Sciences (IPM), Tehran, Iran

H. Bakhshiansohi, H. Behnamian, S.M. Etesami²², A. Fahim²³, R. Goldouzian, M. Khakzad, M. Mohammadi Najafabadi, M. Naseri, S. Paktnat Mehdiabadi, F. Rezaei Hosseinabadi, B. Safarzadeh²⁴, M. Zeinali

University College Dublin, Dublin, Ireland

M. Felcini, M. Grunewald

INFN Sezione di Bari ^a, Università di Bari ^b, Politecnico di Bari ^c, Bari, Italy

M. Abbrescia^{a,b}, L. Barbone^{a,b}, C. Calabria^{a,b}, S.S. Chhibra^{a,b}, A. Colaleo^a, D. Creanza^{a,c}, N. De Filippis^{a,c}, M. De Palma^{a,b}, L. Fiore^a, G. Iaselli^{a,c}, G. Maggi^{a,c}, M. Maggi^a, S. My^{a,c}, S. Nuzzo^{a,b}, A. Pompili^{a,b}, G. Pugliese^{a,c}, R. Radogna^{a,b,2}, G. Selvaggi^{a,b}, L. Silvestris^{a,2}, G. Singh^{a,b}, R. Venditti^{a,b}, G. Zito^a

INFN Sezione di Bologna ^a, Università di Bologna ^b, Bologna, Italy

G. Abbiendi^a, A.C. Benvenuti^a, D. Bonacorsi^{a,b}, S. Braibant-Giacomelli^{a,b}, L. Brigliadori^{a,b}, R. Campanini^{a,b}, P. Capiluppi^{a,b}, A. Castro^{a,b}, F.R. Cavallo^a, G. Codispoti^{a,b}, M. Cuffiani^{a,b}, G.M. Dallavalle^a, F. Fabbri^a, A. Fanfani^{a,b}, D. Fasanella^{a,b}, P. Giacomelli^a, C. Grandi^a, L. Guiducci^{a,b}, S. Marcellini^a, G. Masetti^a, A. Montanari^a, F.L. Navarria^{a,b}, A. Perrotta^a, F. Primavera^{a,b}, A.M. Rossi^{a,b}, T. Rovelli^{a,b}, G.P. Siroli^{a,b}, N. Tosi^{a,b}, R. Travaglini^{a,b}

INFN Sezione di Catania ^a, Università di Catania ^b, CSFNSM ^c, Catania, Italy

S. Albergo^{a,b}, G. Cappello^a, M. Chiorboli^{a,b}, S. Costa^{a,b}, F. Giordano^{a,2}, R. Potenza^{a,b}, A. Tricomi^{a,b}, C. Tuve^{a,b}

INFN Sezione di Firenze ^a, Università di Firenze ^b, Firenze, Italy

G. Barbagli^a, V. Ciulli^{a,b}, C. Civinini^a, R. D'Alessandro^{a,b}, E. Focardi^{a,b}, E. Gallo^a, S. Gonzi^{a,b}, V. Gori^{a,b,2}, P. Lenzi^{a,b}, M. Meschini^a, S. Paoletti^a, G. Sguazzoni^a, A. Tropiano^{a,b}

INFN Laboratori Nazionali di Frascati, Frascati, Italy

L. Benussi, S. Bianco, F. Fabbri, D. Piccolo

INFN Sezione di Genova ^a, Università di Genova ^b, Genova, Italy

R. Ferretti^{a,b}, F. Ferro^a, M. Lo Vetere^{a,b}, E. Robutti^a, S. Tosi^{a,b}

INFN Sezione di Milano-Bicocca ^a, Università di Milano-Bicocca ^b, Milano, Italy

M.E. Dinardo^{a,b}, S. Fiorendi^{a,b,2}, S. Gennai^{a,2}, R. Gerosa², A. Ghezzi^{a,b}, P. Govoni^{a,b}, M.T. Lucchini^{a,b,2}, S. Malvezzi^a, R.A. Manzoni^{a,b}, A. Martelli^{a,b}, B. Marzocchi, D. Menasce^a, L. Moroni^a, M. Paganoni^{a,b}, D. Pedrini^a, S. Ragazzi^{a,b}, N. Redaelli^a, T. Tabarelli de Fatis^{a,b}

INFN Sezione di Napoli ^a, Università di Napoli 'Federico II' ^b, Università della Basilicata (Potenza) ^c, Università G. Marconi (Roma) ^d, Napoli, Italy

S. Buontempo^a, N. Cavallo^{a,c}, S. Di Guida^{a,d,2}, F. Fabozzi^{a,c}, A.O.M. Iorio^{a,b}, L. Lista^a, S. Meola^{a,d,2}, M. Merola^a, P. Paolucci^{a,2}

INFN Sezione di Padova ^a, Università di Padova ^b, Università di Trento (Trento) ^c, Padova, Italy

P. Azzi^a, N. Bacchetta^a, M. Bellato^a, M. Biasotto^{a,25}, A. Branca^{a,b}, R. Carlin^{a,b}, P. Checchia^a, M. Dall'Osso^{a,b}, T. Dorigo^a, F. Fanzago^a, M. Galanti^{a,b}, F. Gasparini^{a,b}, U. Gasparini^{a,b}, P. Giubilato^{a,b}, A. Gozzelino^a, K. Kanishchev^{a,c}, S. Lacaprara^a, M. Margoni^{a,b},

A.T. Meneguzzo^{a,b}, J. Pazzini^{a,b}, N. Pozzobon^{a,b}, P. Ronchese^{a,b}, F. Simonetto^{a,b}, E. Torassa^a, M. Tosi^{a,b}, P. Zotto^{a,b}, A. Zucchetta^{a,b}

INFN Sezione di Pavia ^a, Università di Pavia ^b, Pavia, Italy

M. Gabusi^{a,b}, S.P. Ratti^{a,b}, V. Re^a, C. Riccardi^{a,b}, P. Salvini^a, P. Vitulo^{a,b}

INFN Sezione di Perugia ^a, Università di Perugia ^b, Perugia, Italy

M. Biasini^{a,b}, G.M. Bilei^a, D. Ciangottini^{a,b}, L. Fanò^{a,b}, P. Lariccia^{a,b}, G. Mantovani^{a,b}, M. Menichelli^a, F. Romeo^{a,b}, A. Saha^a, A. Santocchia^{a,b}, A. Spiezia^{a,b,2}

INFN Sezione di Pisa ^a, Università di Pisa ^b, Scuola Normale Superiore di Pisa ^c, Pisa, Italy

K. Androsov^{a,26}, P. Azzurri^a, G. Bagliesi^a, J. Bernardini^a, T. Boccali^a, G. Broccolo^{a,c}, R. Castaldi^a, M.A. Ciocci^{a,26}, R. Dell'Orso^a, S. Donato^{a,c}, F. Fiori^{a,c}, L. Foà^{a,c}, A. Giassi^a, M.T. Grippo^{a,26}, F. Ligabue^{a,c}, T. Lomtadze^a, L. Martini^{a,b}, A. Messineo^{a,b}, C.S. Moon^{a,27}, F. Palla^{a,2}, A. Rizzi^{a,b}, A. Savoy-Navarro^{a,28}, A.T. Serban^a, P. Spagnolo^a, P. Squillaciotti^{a,26}, R. Tenchini^a, G. Tonelli^{a,b}, A. Venturi^a, P.G. Verdini^a, C. Vernier^{a,c,2}

INFN Sezione di Roma ^a, Università di Roma ^b, Roma, Italy

L. Barone^{a,b}, F. Cavallari^a, G. D'imperio^{a,b}, D. Del Re^{a,b}, M. Diemoz^a, M. Grassi^{a,b}, C. Jorda^a, E. Longo^{a,b}, F. Margaroli^{a,b}, P. Meridiani^a, F. Micheli^{a,b,2}, S. Nourbakhsh^{a,b}, G. Organtini^{a,b}, R. Paramatti^a, S. Rahatlou^{a,b}, C. Rovelli^a, F. Santanastasio^{a,b}, L. Soffi^{a,b,2}, P. Traczyk^{a,b}

INFN Sezione di Torino ^a, Università di Torino ^b, Università del Piemonte Orientale (Novara) ^c, Torino, Italy

N. Amapane^{a,b}, R. Arcidiacono^{a,c}, S. Argiro^{a,b,2}, M. Arneodo^{a,c}, R. Bellan^{a,b}, C. Biino^a, N. Cartiglia^a, S. Casasso^{a,b,2}, M. Costa^{a,b}, A. Degano^{a,b}, N. Demaria^a, L. Finco^{a,b}, C. Mariotti^a, S. Maselli^a, E. Migliore^{a,b}, V. Monaco^{a,b}, M. Musich^a, M.M. Obertino^{a,c,2}, G. Ortona^{a,b}, L. Pacher^{a,b}, N. Pastrone^a, M. Pelliccioni^a, G.L. Pinna Angioni^{a,b}, A. Potenza^{a,b}, A. Romero^{a,b}, M. Ruspa^{a,c}, R. Sacchi^{a,b}, A. Solano^{a,b}, A. Staiano^a, U. Tamponi^a

INFN Sezione di Trieste ^a, Università di Trieste ^b, Trieste, Italy

S. Belforte^a, V. Candelise^{a,b}, M. Casarsa^a, F. Cossutti^a, G. Della Ricca^{a,b}, B. Gobbo^a, C. La Licata^{a,b}, M. Marone^{a,b}, A. Schizzi^{a,b,2}, T. Umer^{a,b}, A. Zanetti^a

Kangwon National University, Chunchon, Korea

S. Chang, A. Kropivnitskaya, S.K. Nam

Kyungpook National University, Daegu, Korea

D.H. Kim, G.N. Kim, M.S. Kim, D.J. Kong, S. Lee, Y.D. Oh, H. Park, A. Sakharov, D.C. Son

Chonbuk National University, Jeonju, Korea

T.J. Kim

Chonnam National University, Institute for Universe and Elementary Particles, Kwangju, Korea

J.Y. Kim, S. Song

Korea University, Seoul, Korea

S. Choi, D. Gyun, B. Hong, M. Jo, H. Kim, Y. Kim, B. Lee, K.S. Lee, S.K. Park, Y. Roh

University of Seoul, Seoul, Korea

M. Choi, J.H. Kim, I.C. Park, G. Ryu, M.S. Ryu

Sungkyunkwan University, Suwon, Korea

Y. Choi, Y.K. Choi, J. Goh, D. Kim, E. Kwon, J. Lee, H. Seo, I. Yu

Vilnius University, Vilnius, Lithuania
A. Juodagalvis

National Centre for Particle Physics, Universiti Malaya, Kuala Lumpur, Malaysia
J.R. Komaragiri, M.A.B. Md Ali

Centro de Investigacion y de Estudios Avanzados del IPN, Mexico City, Mexico
H. Castilla-Valdez, E. De La Cruz-Burelo, I. Heredia-de La Cruz²⁹, A. Hernandez-Almada,
R. Lopez-Fernandez, A. Sanchez-Hernandez

Universidad Iberoamericana, Mexico City, Mexico
S. Carrillo Moreno, F. Vazquez Valencia

Benemerita Universidad Autonoma de Puebla, Puebla, Mexico
I. Pedraza, H.A. Salazar Ibarguen

Universidad Autónoma de San Luis Potosí, San Luis Potosí, Mexico
E. Casimiro Linares, A. Morelos Pineda

University of Auckland, Auckland, New Zealand
D. Kofcheck

University of Canterbury, Christchurch, New Zealand
P.H. Butler, S. Reucroft

National Centre for Physics, Quaid-I-Azam University, Islamabad, Pakistan
A. Ahmad, M. Ahmad, Q. Hassan, H.R. Hoorani, S. Khalid, W.A. Khan, T. Khurshid,
M.A. Shah, M. Shoib

National Centre for Nuclear Research, Swierk, Poland
H. Bialkowska, M. Bluj, B. Boimska, T. Frueboes, M. Górski, M. Kazana, K. Nawrocki,
K. Romanowska-Rybinska, M. Szleper, P. Zalewski

Institute of Experimental Physics, Faculty of Physics, University of Warsaw, Warsaw, Poland
G. Brona, K. Bunkowski, M. Cwiok, W. Dominik, K. Doroba, A. Kalinowski, M. Konecki,
J. Krolikowski, M. Misiura, M. Olszewski, W. Wolszczak

Laboratório de Instrumentação e Física Experimental de Partículas, Lisboa, Portugal
P. Bargassa, C. Beirão Da Cruz E Silva, P. Faccioli, P.G. Ferreira Parracho, M. Gallinaro, L. Lloret
Iglesias, F. Nguyen, J. Rodrigues Antunes, J. Seixas, J. Varela, P. Vischia

Joint Institute for Nuclear Research, Dubna, Russia
S. Afanasiev, P. Bunin, M. Gavrilenco, I. Golutvin, I. Gorbunov, A. Kamenev, V. Karjavin,
V. Konoplyanikov, A. Lanev, A. Malakhov, V. Matveev³⁰, P. Moisenz, V. Palichik, V. Perelygin,
S. Shmatov, N. Skatchkov, V. Smirnov, A. Zarubin

Petersburg Nuclear Physics Institute, Gatchina (St. Petersburg), Russia
V. Golovtsov, Y. Ivanov, V. Kim³¹, P. Levchenko, V. Murzin, V. Oreshkin, I. Smirnov, V. Sulimov,
L. Uvarov, S. Vavilov, A. Vorobyev, An. Vorobyev

Institute for Nuclear Research, Moscow, Russia
Yu. Andreev, A. Dermenev, S. Gninenko, N. Golubev, M. Kirsanov, N. Krasnikov, A. Pashenkov,
D. Tlisov, A. Toropin

Institute for Theoretical and Experimental Physics, Moscow, Russia
V. Epshteyn, V. Gavrilov, N. Lychkovskaya, V. Popov, G. Safronov, S. Semenov, A. Spiridonov,
V. Stolin, E. Vlasov, A. Zhokin

P.N. Lebedev Physical Institute, Moscow, Russia

V. Andreev, M. Azarkin, I. Dremin, M. Kirakosyan, A. Leonidov, G. Mesyats, S.V. Rusakov, A. Vinogradov

Skobeltsyn Institute of Nuclear Physics, Lomonosov Moscow State University, Moscow, Russia

A. Belyaev, E. Boos, A. Ershov, A. Gribushin, V. Klyukhin, O. Kodolova, V. Korotkikh, I. Lokhtin, S. Obraztsov, S. Petrushanko, V. Savrin, A. Snigirev, I. Vardanyan

State Research Center of Russian Federation, Institute for High Energy Physics, Protvino, Russia

I. Azhgirey, I. Bayshev, S. Bitioukov, V. Kachanov, A. Kalinin, D. Konstantinov, V. Krychkine, V. Petrov, R. Ryutin, A. Sobol, L. Tourtchanovitch, S. Troshin, N. Tyurin, A. Uzunian, A. Volkov

University of Belgrade, Faculty of Physics and Vinca Institute of Nuclear Sciences, Belgrade, Serbia

P. Adzic³², M. Ekmedzic, J. Milosevic, V. Rekovic

Centro de Investigaciones Energéticas Medioambientales y Tecnológicas (CIEMAT), Madrid, Spain

J. Alcaraz Maestre, C. Battilana, E. Calvo, M. Cerrada, M. Chamizo Llatas, N. Colino, B. De La Cruz, A. Delgado Peris, D. Domínguez Vázquez, A. Escalante Del Valle, C. Fernandez Bedoya, J.P. Fernández Ramos, J. Flix, M.C. Fouz, P. Garcia-Abia, O. Gonzalez Lopez, S. Goy Lopez, J.M. Hernandez, M.I. Josa, E. Navarro De Martino, A. Pérez-Calero Yzquierdo, J. Puerta Pelayo, A. Quintario Olmeda, I. Redondo, L. Romero, M.S. Soares

Universidad Autónoma de Madrid, Madrid, Spain

C. Albajar, J.F. de Trocóniz, M. Missiroli, D. Moran

Universidad de Oviedo, Oviedo, Spain

H. Brun, J. Cuevas, J. Fernandez Menendez, S. Folgueras, I. Gonzalez Caballero

Instituto de Física de Cantabria (IFCA), CSIC-Universidad de Cantabria, Santander, Spain

J.A. Brochero Cifuentes, I.J. Cabrillo, A. Calderon, J. Duarte Campderros, M. Fernandez, G. Gomez, A. Graziano, A. Lopez Virto, J. Marco, R. Marco, C. Martinez Rivero, F. Matorras, F.J. Munoz Sanchez, J. Piedra Gomez, T. Rodrigo, A.Y. Rodríguez-Marrero, A. Ruiz-Jimeno, L. Scodellaro, I. Vila, R. Vilar Cortabitarte

CERN, European Organization for Nuclear Research, Geneva, Switzerland

D. Abbaneo, E. Auffray, G. Auzinger, M. Bachtis, P. Baillon, A.H. Ball, D. Barney, A. Benaglia, J. Bendavid, L. Benhabib, J.F. Benitez, C. Bernet⁷, G. Bianchi, P. Bloch, A. Bocci, A. Bonato, O. Bondu, C. Botta, H. Breuker, T. Camporesi, G. Cerminara, S. Colafranceschi³³, M. D'Alfonso, D. d'Enterria, A. Dabrowski, A. David, F. De Guio, A. De Roeck, S. De Visscher, E. Di Marco, M. Dobson, M. Dordevic, N. Dupont-Sagorin, A. Elliott-Peisert, J. Eugster, G. Franzoni, W. Funk, D. Gigi, K. Gill, D. Giordano, M. Girone, F. Glege, R. Guida, S. Gundacker, M. Guthoff, J. Hammer, M. Hansen, P. Harris, J. Hegeman, V. Innocente, P. Janot, K. Kousouris, K. Krajczar, P. Lecoq, C. Lourenço, N. Magini, L. Malgeri, M. Mannelli, J. Marrouche, L. Masetti, F. Meijers, S. Mersi, E. Meschi, F. Moortgat, S. Morovic, M. Mulders, P. Musella, L. Orsini, L. Pape, E. Perez, L. Perrozzi, A. Petrilli, G. Petrucciani, A. Pfeiffer, M. Pierini, M. Pimiä, D. Piparo, M. Plagge, A. Racz, G. Rolandi³⁴, M. Rovere, H. Sakulin, C. Schäfer, C. Schwick, A. Sharma, P. Siegrist, P. Silva, M. Simon, P. Sphicas³⁵, D. Spiga, J. Steggemann, B. Stieger, M. Stoye, Y. Takahashi, D. Treille, A. Tsirou, G.I. Veres¹⁷, J.R. Vlimant, N. Wardle, H.K. Wöhri, H. Wollny, W.D. Zeuner

Paul Scherrer Institut, Villigen, Switzerland

W. Bertl, K. Deiters, W. Erdmann, R. Horisberger, Q. Ingram, H.C. Kaestli, D. Kotlinski, U. Langenegger, D. Renker, T. Rohe

Institute for Particle Physics, ETH Zurich, Zurich, Switzerland

F. Bachmair, L. Bäni, L. Bianchini, M.A. Buchmann, B. Casal, N. Chanon, G. Dissertori, M. Dittmar, M. Donegà, M. Dünser, P. Eller, C. Grab, D. Hits, J. Hoss, W. Lustermann, B. Mangano, A.C. Marini, P. Martinez Ruiz del Arbol, M. Masciovecchio, D. Meister, N. Mohr, C. Nägeli³⁶, F. Nessi-Tedaldi, F. Pandolfi, F. Pauss, M. Peruzzi, M. Quittnat, L. Rebane, M. Rossini, A. Starodumov³⁷, M. Takahashi, K. Theofilatos, R. Wallny, H.A. Weber

Universität Zürich, Zurich, Switzerland

C. Amsler³⁸, M.F. Canelli, V. Chiochia, A. De Cosa, A. Hinzmann, T. Hreus, B. Kilminster, C. Lange, B. Millan Mejias, J. Ngadiuba, P. Robmann, F.J. Ronga, S. Taroni, M. Verzetti, Y. Yang

National Central University, Chung-Li, Taiwan

M. Cardaci, K.H. Chen, C. Ferro, C.M. Kuo, W. Lin, Y.J. Lu, R. Volpe, S.S. Yu

National Taiwan University (NTU), Taipei, Taiwan

P. Chang, Y.H. Chang, Y.W. Chang, Y. Chao, K.F. Chen, P.H. Chen, C. Dietz, U. Grundler, W.-S. Hou, K.Y. Kao, Y.J. Lei, Y.F. Liu, R.-S. Lu, D. Majumder, E. Petrakou, Y.M. Tzeng, R. Wilken

Chulalongkorn University, Faculty of Science, Department of Physics, Bangkok, Thailand

B. Asavapibhop, N. Srimanobhas, N. Suwonjandee

Cukurova University, Adana, Turkey

A. Adiguzel, M.N. Bakirci³⁹, S. Cerci⁴⁰, C. Dozen, I. Dumanoglu, E. Eskut, S. Girgis, G. Gokbulut, E. Gurpinar, I. Hos, E.E. Kangal, A. Kayis Topaksu, G. Onengut⁴¹, K. Ozdemir, S. Ozturk³⁹, A. Polatoz, D. Sunar Cerci⁴⁰, B. Tali⁴⁰, H. Topakli³⁹, M. Vergili

Middle East Technical University, Physics Department, Ankara, Turkey

I.V. Akin, B. Bilin, S. Bilmis, H. Gamsizkan⁴², G. Karapinar⁴³, K. Ocalan⁴⁴, S. Sekmen, U.E. Surat, M. Yalvac, M. Zeyrek

Bogazici University, Istanbul, Turkey

E. Gürmez, B. Isildak⁴⁵, M. Kaya⁴⁶, O. Kaya⁴⁷

Istanbul Technical University, Istanbul, Turkey

K. Cankocak, F.I. Vardarli

National Scientific Center, Kharkov Institute of Physics and Technology, Kharkov, Ukraine

L. Levchuk, P. Sorokin

University of Bristol, Bristol, United Kingdom

J.J. Brooke, E. Clement, D. Cussans, H. Flacher, R. Frazier, J. Goldstein, M. Grimes, G.P. Heath, H.F. Heath, J. Jacob, L. Kreczko, C. Lucas, Z. Meng, D.M. Newbold⁴⁸, S. Paramesvaran, A. Poll, S. Senkin, V.J. Smith, T. Williams

Rutherford Appleton Laboratory, Didcot, United Kingdom

A. Belyaev⁴⁹, C. Brew, R.M. Brown, D.J.A. Cockerill, J.A. Coughlan, K. Harder, S. Harper, E. Olaiya, D. Pettyt, C.H. Shepherd-Themistocleous, A. Thea, I.R. Tomalin, W.J. Womersley, S.D. Worm

Imperial College, London, United Kingdom

M. Baber, R. Bainbridge, O. Buchmuller, D. Burton, D. Colling, N. Cripps, M. Cutajar, P. Dauncey, G. Davies, M. Della Negra, P. Dunne, W. Ferguson, J. Fulcher, D. Futyan, A. Gilbert,

G. Hall, G. Iles, M. Jarvis, G. Karapostoli, M. Kenzie, R. Lane, R. Lucas⁴⁸, L. Lyons, A.-M. Magnan, S. Malik, B. Mathias, J. Nash, A. Nikitenko³⁷, J. Pela, M. Pesaresi, K. Petridis, D.M. Raymond, S. Rogerson, A. Rose, C. Seez, P. Sharp[†], A. Tapper, M. Vazquez Acosta, T. Virdee, S.C. Zenz

Brunel University, Uxbridge, United Kingdom

J.E. Cole, P.R. Hobson, A. Khan, P. Kyberd, D. Leggat, D. Leslie, W. Martin, I.D. Reid, P. Symonds, L. Teodorescu, M. Turner

Baylor University, Waco, USA

J. Dittmann, K. Hatakeyama, A. Kasmi, H. Liu, T. Scarborough

The University of Alabama, Tuscaloosa, USA

O. Charaf, S.I. Cooper, C. Henderson, P. Rumerio

Boston University, Boston, USA

A. Avetisyan, T. Bose, C. Fantasia, P. Lawson, C. Richardson, J. Rohlf, J. St. John, L. Sulak

Brown University, Providence, USA

J. Alimena, E. Berry, S. Bhattacharya, G. Christopher, D. Cutts, Z. Demiragli, N. Dhingra, A. Ferapontov, A. Garabedian, U. Heintz, G. Kukartsev, E. Laird, G. Landsberg, M. Luk, M. Narain, M. Segala, T. Sinthuprasith, T. Speer, J. Swanson

University of California, Davis, Davis, USA

R. Breedon, G. Breto, M. Calderon De La Barca Sanchez, S. Chauhan, M. Chertok, J. Conway, R. Conway, P.T. Cox, R. Erbacher, M. Gardner, W. Ko, R. Lander, T. Miceli, M. Mulhearn, D. Pellett, J. Pilot, F. Ricci-Tam, M. Searle, S. Shalhout, J. Smith, M. Squires, D. Stolp, M. Tripathi, S. Wilbur, R. Yohay

University of California, Los Angeles, USA

R. Cousins, P. Everaerts, C. Farrell, J. Hauser, M. Ignatenko, G. Rakness, E. Takasugi, V. Valuev, M. Weber

University of California, Riverside, Riverside, USA

K. Burt, R. Clare, J. Ellison, J.W. Gary, G. Hanson, J. Heilman, M. Ivova Rikova, P. Jandir, E. Kennedy, F. Lacroix, O.R. Long, A. Luthra, M. Malberti, H. Nguyen, M. Olmedo Negrete, A. Shrinivas, S. Sumowidagdo, S. Wimpenny

University of California, San Diego, La Jolla, USA

W. Andrews, J.G. Branson, G.B. Cerati, S. Cittolin, R.T. D'Agnolo, D. Evans, A. Holzner, R. Kelley, D. Klein, M. Lebourgeois, J. Letts, I. Macneill, D. Olivito, S. Padhi, C. Palmer, M. Pieri, M. Sani, V. Sharma, S. Simon, E. Sudano, M. Tadel, Y. Tu, A. Vartak, C. Welke, F. Würthwein, A. Yagil

University of California, Santa Barbara, Santa Barbara, USA

D. Barge, J. Bradmiller-Feld, C. Campagnari, T. Danielson, A. Dishaw, K. Flowers, M. Franco Sevilla, P. Geffert, C. George, F. Golf, L. Gouskos, J. Incandela, C. Justus, N. Mccoll, J. Richman, D. Stuart, W. To, C. West, J. Yoo

California Institute of Technology, Pasadena, USA

A. Apresyan, A. Bornheim, J. Bunn, Y. Chen, J. Duarte, A. Mott, H.B. Newman, C. Pena, C. Rogan, M. Spiropulu, V. Timciuc, R. Wilkinson, S. Xie, R.Y. Zhu

Carnegie Mellon University, Pittsburgh, USA

V. Azzolini, A. Calamba, B. Carlson, T. Ferguson, Y. Iiyama, M. Paulini, J. Russ, H. Vogel, I. Vorobiev

University of Colorado at Boulder, Boulder, USA

J.P. Cumalat, W.T. Ford, A. Gaz, E. Luiggi Lopez, U. Nauenberg, J.G. Smith, K. Stenson, K.A. Ulmer, S.R. Wagner

Cornell University, Ithaca, USA

J. Alexander, A. Chatterjee, J. Chu, S. Dittmer, N. Eggert, N. Mirman, G. Nicolas Kaufman, J.R. Patterson, A. Ryd, E. Salvati, L. Skinnari, W. Sun, W.D. Teo, J. Thom, J. Thompson, J. Tucker, Y. Weng, L. Winstrom, P. Wittich

Fairfield University, Fairfield, USA

D. Winn

Fermi National Accelerator Laboratory, Batavia, USA

S. Abdullin, M. Albrow, J. Anderson, G. Apollinari, L.A.T. Bauerick, A. Beretvas, J. Berryhill, P.C. Bhat, G. Bolla, K. Burkett, J.N. Butler, H.W.K. Cheung, F. Chlebana, S. Cihangir, V.D. Elvira, I. Fisk, J. Freeman, Y. Gao, E. Gottschalk, L. Gray, D. Green, S. Grünendahl, O. Gutsche, J. Hanlon, D. Hare, R.M. Harris, J. Hirschauer, B. Hooberman, S. Jindariani, M. Johnson, U. Joshi, K. Kaadze, B. Klima, B. Kreis, S. Kwan, J. Linacre, D. Lincoln, R. Lipton, T. Liu, J. Lykken, K. Maeshima, J.M. Marraffino, V.I. Martinez Outschoorn, S. Maruyama, D. Mason, P. McBride, P. Merkel, K. Mishra, S. Mrenna, Y. Musienko³⁰, S. Nahn, C. Newman-Holmes, V. O'Dell, O. Prokofyev, E. Sexton-Kennedy, S. Sharma, A. Soha, W.J. Spalding, L. Spiegel, L. Taylor, S. Tkaczyk, N.V. Tran, L. Uplegger, E.W. Vaandering, R. Vidal, A. Whitbeck, J. Whitmore, F. Yang

University of Florida, Gainesville, USA

D. Acosta, P. Avery, P. Bortignon, D. Bourilkov, M. Carver, T. Cheng, D. Curry, S. Das, M. De Gruttola, G.P. Di Giovanni, R.D. Field, M. Fisher, I.K. Furic, J. Hugon, J. Konigsberg, A. Korytov, T. Kypreos, J.F. Low, K. Matchev, P. Milenovic⁵⁰, G. Mitselmakher, L. Muniz, A. Rinkevicius, L. Shchutska, M. Snowball, D. Sperka, J. Yelton, M. Zakaria

Florida International University, Miami, USA

S. Hewamanage, S. Linn, P. Markowitz, G. Martinez, J.L. Rodriguez

Florida State University, Tallahassee, USA

T. Adams, A. Askew, J. Bochenek, B. Diamond, J. Haas, S. Hagopian, V. Hagopian, K.F. Johnson, H. Prosper, V. Veeraraghavan, M. Weinberg

Florida Institute of Technology, Melbourne, USA

M.M. Baarmann, M. Hohlmann, H. Kalakhety, F. Yumiceva

University of Illinois at Chicago (UIC), Chicago, USA

M.R. Adams, L. Apanasevich, V.E. Bazterra, D. Berry, R.R. Betts, I. Bucinskaite, R. Cavanaugh, O. Evdokimov, L. Gauthier, C.E. Gerber, D.J. Hofman, S. Khalatyan, P. Kurt, D.H. Moon, C. O'Brien, C. Silkworth, P. Turner, N. Varelas

The University of Iowa, Iowa City, USA

E.A. Albayrak⁵¹, B. Bilki⁵², W. Clarida, K. Dilsiz, F. Duru, M. Haytmyradov, J.-P. Merlo, H. Mermerkaya⁵³, A. Mestvirishvili, A. Moeller, J. Nachtman, H. Ogul, Y. Onel, F. Ozok⁵¹, A. Penzo, R. Rahmat, S. Sen, P. Tan, E. Tiras, J. Wetzel, T. Yetkin⁵⁴, K. Yi

Johns Hopkins University, Baltimore, USA

B.A. Barnett, B. Blumenfeld, S. Bolognesi, D. Fehling, A.V. Gritsan, P. Maksimovic, C. Martin, M. Swartz

The University of Kansas, Lawrence, USA

P. Baringer, A. Bean, G. Benelli, C. Bruner, R.P. Kenny III, M. Malek, M. Murray, D. Noonan, S. Sanders, J. Sekaric, R. Stringer, Q. Wang, J.S. Wood

Kansas State University, Manhattan, USA

A.F. Barfuss, I. Chakaberia, A. Ivanov, S. Khalil, M. Makouski, Y. Maravin, L.K. Saini, S. Shrestha, N. Skhirtladze, I. Svintradze

Lawrence Livermore National Laboratory, Livermore, USA

J. Gronberg, D. Lange, F. Rebassoo, D. Wright

University of Maryland, College Park, USA

A. Baden, A. Belloni, B. Calvert, S.C. Eno, J.A. Gomez, N.J. Hadley, R.G. Kellogg, T. Kolberg, Y. Lu, M. Marionneau, A.C. Mignerey, K. Pedro, A. Skuja, M.B. Tonjes, S.C. Tonwar

Massachusetts Institute of Technology, Cambridge, USA

A. Apyan, R. Barbieri, G. Bauer, W. Busza, I.A. Cali, M. Chan, L. Di Matteo, V. Dutta, G. Gomez Ceballos, M. Goncharov, D. Gulhan, M. Klute, Y.S. Lai, Y.-J. Lee, A. Levin, P.D. Luckey, T. Ma, C. Paus, D. Ralph, C. Roland, G. Roland, G.S.F. Stephans, F. Stöckli, K. Sumorok, D. Velicanu, J. Veverka, B. Wyslouch, M. Yang, M. Zanetti, V. Zhukova

University of Minnesota, Minneapolis, USA

B. Dahmes, A. Gude, S.C. Kao, K. Klapoetke, Y. Kubota, J. Mans, N. Pastika, R. Rusack, A. Singovsky, N. Tambe, J. Turkewitz

University of Mississippi, Oxford, USA

J.G. Acosta, S. Oliveros

University of Nebraska-Lincoln, Lincoln, USA

E. Avdeeva, K. Bloom, S. Bose, D.R. Claes, A. Dominguez, R. Gonzalez Suarez, J. Keller, D. Knowlton, I. Kravchenko, J. Lazo-Flores, S. Malik, F. Meier, G.R. Snow, M. Zvada

State University of New York at Buffalo, Buffalo, USA

J. Dolen, A. Godshalk, I. Iashvili, A. Kharchilava, A. Kumar, S. Rappoccio

Northeastern University, Boston, USA

G. Alverson, E. Barberis, D. Baumgartel, M. Chasco, J. Haley, A. Massironi, D.M. Morse, D. Nash, T. Orimoto, D. Trocino, R.-J. Wang, D. Wood, J. Zhang

Northwestern University, Evanston, USA

K.A. Hahn, A. Kubik, N. Mucia, N. Odell, B. Pollack, A. Pozdnyakov, M. Schmitt, S. Stoynev, K. Sung, M. Velasco, S. Won

University of Notre Dame, Notre Dame, USA

A. Brinkerhoff, K.M. Chan, A. Drozdetskiy, M. Hildreth, C. Jessop, D.J. Karmgard, N. Kellams, K. Lannon, W. Luo, S. Lynch, N. Marinelli, T. Pearson, M. Planer, R. Ruchti, N. Valls, M. Wayne, M. Wolf, A. Woodard

The Ohio State University, Columbus, USA

L. Antonelli, J. Brinson, B. Bylsma, L.S. Durkin, S. Flowers, C. Hill, R. Hughes, K. Kotov, T.Y. Ling, D. Puigh, M. Rodenburg, G. Smith, B.L. Winer, H. Wolfe, H.W. Wulsin

Princeton University, Princeton, USA

O. Driga, P. Elmer, P. Hebda, A. Hunt, S.A. Koay, P. Lujan, D. Marlow, T. Medvedeva, M. Mooney, J. Olsen, P. Piroué, X. Quan, H. Saka, D. Stickland², C. Tully, J.S. Werner, A. Zuranski

University of Puerto Rico, Mayaguez, USA

E. Brownson, H. Mendez, J.E. Ramirez Vargas

Purdue University, West Lafayette, USA

V.E. Barnes, D. Benedetti, D. Bortoletto, M. De Mattia, L. Gutay, Z. Hu, M.K. Jha, M. Jones, K. Jung, M. Kress, N. Leonardo, D. Lopes Pegna, V. Maroussov, D.H. Miller, N. Neumeister, B.C. Radburn-Smith, X. Shi, I. Shipsey, D. Silvers, A. Svyatkovskiy, F. Wang, W. Xie, L. Xu, H.D. Yoo, J. Zablocki, Y. Zheng

Purdue University Calumet, Hammond, USA

N. Parashar, J. Stupak

Rice University, Houston, USA

A. Adair, B. Akgun, K.M. Ecklund, F.J.M. Geurts, W. Li, B. Michlin, B.P. Padley, R. Redjimi, J. Roberts, J. Zabel

University of Rochester, Rochester, USA

B. Betchart, A. Bodek, R. Covarelli, P. de Barbaro, R. Demina, Y. Eshaq, T. Ferbel, A. Garcia-Bellido, P. Goldenzweig, J. Han, A. Harel, A. Khukhunaishvili, G. Petrillo, D. Vishnevskiy

The Rockefeller University, New York, USA

R. Ciesielski, L. Demortier, K. Goulian, G. Lungu, C. Mesropian

Rutgers, The State University of New Jersey, Piscataway, USA

S. Arora, A. Barker, J.P. Chou, C. Contreras-Campana, E. Contreras-Campana, D. Duggan, D. Ferencek, Y. Gershtein, R. Gray, E. Halkiadakis, D. Hidas, S. Kaplan, A. Lath, S. Panwalkar, M. Park, R. Patel, S. Salur, S. Schnetzer, S. Somalwar, R. Stone, S. Thomas, P. Thomassen, M. Walker

University of Tennessee, Knoxville, USA

K. Rose, S. Spanier, A. York

Texas A&M University, College Station, USA

O. Bouhali⁵⁵, A. Castaneda Hernandez, R. Eusebi, W. Flanagan, J. Gilmore, T. Kamon⁵⁶, V. Khotilovich, V. Krutelyov, R. Montalvo, I. Osipenkov, Y. Pakhotin, A. Perloff, J. Roe, A. Rose, A. Safonov, T. Sakuma, I. Suarez, A. Tatarinov

Texas Tech University, Lubbock, USA

N. Akchurin, C. Cowden, J. Damgov, C. Dragoiu, P.R. Dudero, J. Faulkner, K. Kovitanggoon, S. Kunori, S.W. Lee, T. Libeiro, I. Volobouev

Vanderbilt University, Nashville, USA

E. Appelt, A.G. Delannoy, S. Greene, A. Gurrola, W. Johns, C. Maguire, Y. Mao, A. Melo, M. Sharma, P. Sheldon, B. Snook, S. Tuo, J. Velkovska

University of Virginia, Charlottesville, USA

M.W. Arenton, S. Boutle, B. Cox, B. Francis, J. Goodell, R. Hirosky, A. Ledovskoy, H. Li, C. Lin, C. Neu, J. Wood

Wayne State University, Detroit, USA

C. Clarke, R. Harr, P.E. Karchin, C. Kottachchi Kankanamge Don, P. Lamichhane, J. Sturdy

University of Wisconsin, Madison, USA

D.A. Belknap, D. Carlsmith, M. Cepeda, S. Dasu, L. Dodd, S. Duric, E. Friis, R. Hall-Wilton, M. Herndon, A. Hervé, P. Klabbers, A. Lanaro, C. Lazaridis, A. Levine, R. Loveless, A. Mohapatra, I. Ojalvo, T. Perry, G.A. Pierro, G. Polese, I. Ross, T. Sarangi, A. Savin, W.H. Smith, D. Taylor, P. Verwilligen, C. Vuosalo, N. Woods

†: Deceased

- 1: Also at Vienna University of Technology, Vienna, Austria
- 2: Also at CERN, European Organization for Nuclear Research, Geneva, Switzerland
- 3: Also at Institut Pluridisciplinaire Hubert Curien, Université de Strasbourg, Université de Haute Alsace Mulhouse, CNRS/IN2P3, Strasbourg, France
- 4: Also at National Institute of Chemical Physics and Biophysics, Tallinn, Estonia
- 5: Also at Skobeltsyn Institute of Nuclear Physics, Lomonosov Moscow State University, Moscow, Russia
- 6: Also at Universidade Estadual de Campinas, Campinas, Brazil
- 7: Also at Laboratoire Leprince-Ringuet, Ecole Polytechnique, IN2P3-CNRS, Palaiseau, France
- 8: Also at Joint Institute for Nuclear Research, Dubna, Russia
- 9: Also at Suez University, Suez, Egypt
- 10: Also at Cairo University, Cairo, Egypt
- 11: Also at Fayoum University, El-Fayoum, Egypt
- 12: Also at British University in Egypt, Cairo, Egypt
- 13: Now at Ain Shams University, Cairo, Egypt
- 14: Also at Université de Haute Alsace, Mulhouse, France
- 15: Also at Brandenburg University of Technology, Cottbus, Germany
- 16: Also at Institute of Nuclear Research ATOMKI, Debrecen, Hungary
- 17: Also at Eötvös Loránd University, Budapest, Hungary
- 18: Also at University of Debrecen, Debrecen, Hungary
- 19: Also at University of Visva-Bharati, Santiniketan, India
- 20: Now at King Abdulaziz University, Jeddah, Saudi Arabia
- 21: Also at University of Ruhuna, Matara, Sri Lanka
- 22: Also at Isfahan University of Technology, Isfahan, Iran
- 23: Also at Sharif University of Technology, Tehran, Iran
- 24: Also at Plasma Physics Research Center, Science and Research Branch, Islamic Azad University, Tehran, Iran
- 25: Also at Laboratori Nazionali di Legnaro dell'INFN, Legnaro, Italy
- 26: Also at Università degli Studi di Siena, Siena, Italy
- 27: Also at Centre National de la Recherche Scientifique (CNRS) - IN2P3, Paris, France
- 28: Also at Purdue University, West Lafayette, USA
- 29: Also at Universidad Michoacana de San Nicolas de Hidalgo, Morelia, Mexico
- 30: Also at Institute for Nuclear Research, Moscow, Russia
- 31: Also at St. Petersburg State Polytechnical University, St. Petersburg, Russia
- 32: Also at Faculty of Physics, University of Belgrade, Belgrade, Serbia
- 33: Also at Facoltà Ingegneria, Università di Roma, Roma, Italy
- 34: Also at Scuola Normale e Sezione dell'INFN, Pisa, Italy
- 35: Also at University of Athens, Athens, Greece
- 36: Also at Paul Scherrer Institut, Villigen, Switzerland
- 37: Also at Institute for Theoretical and Experimental Physics, Moscow, Russia
- 38: Also at Albert Einstein Center for Fundamental Physics, Bern, Switzerland
- 39: Also at Gaziosmanpasa University, Tokat, Turkey
- 40: Also at Adiyaman University, Adiyaman, Turkey

- 41: Also at Cag University, Mersin, Turkey
- 42: Also at Anadolu University, Eskisehir, Turkey
- 43: Also at Izmir Institute of Technology, Izmir, Turkey
- 44: Also at Necmettin Erbakan University, Konya, Turkey
- 45: Also at Ozyegin University, Istanbul, Turkey
- 46: Also at Marmara University, Istanbul, Turkey
- 47: Also at Kafkas University, Kars, Turkey
- 48: Also at Rutherford Appleton Laboratory, Didcot, United Kingdom
- 49: Also at School of Physics and Astronomy, University of Southampton, Southampton, United Kingdom
- 50: Also at University of Belgrade, Faculty of Physics and Vinca Institute of Nuclear Sciences, Belgrade, Serbia
- 51: Also at Mimar Sinan University, Istanbul, Istanbul, Turkey
- 52: Also at Argonne National Laboratory, Argonne, USA
- 53: Also at Erzincan University, Erzincan, Turkey
- 54: Also at Yildiz Technical University, Istanbul, Turkey
- 55: Also at Texas A&M University at Qatar, Doha, Qatar
- 56: Also at Kyungpook National University, Daegu, Korea